

Optimal Reflection Coefficients for ASK Modulated Backscattering from Passive Tags

Amus Chee Yuen Goay, *Student Member, IEEE*, Deepak Mishra, *Senior Member, IEEE*, Aruna Seneviratne, *Senior Member, IEEE*

Abstract—A passive backscatter tag is an energy-efficient wireless communication device that is ideal for low-power and low-bandwidth applications, such as sensing and identification. Despite their usefulness, the effectiveness of these tags is limited by the amount of energy they can harness from the incident radio signals used to backscatter their information through the modulation of reflections. This paper aims to maximize this harvested power at a passive tag by optimally designing the underlying M-ary amplitude-shift keying (ASK) modulator in a monostatic backscatter communication (BackCom) system. Specifically, we derive the closed-form expression for the global optimal reflection coefficients that maximize the tag’s harvested power while satisfying the minimum symbol error rate (SER) requirement, tag sensitivity, and reader sensitivity constraints. We also proposed optimal binary-ASK modulation design to gain novel design insights on practical BackCom systems with readers having superior sensitivity. We have validated these nontrivial analytical claims via extensive simulations. The numerical results provide insight into the impact of the transmit symbol probability, tag sensitivity constraint, and SER on the maximum average harvested power. Remarkably, our design achieves an overall gain of around 13% over the benchmark, signifying its utility in improving the efficiency of BackCom systems.

Index Terms—Backscattering, Passive Tag, Reflection Coefficient, RFID, ASK, Energy Optimization, SER.

I. INTRODUCTION

Backscatter communication (BackCom) is a low-power, low-cost wireless technique for tags that reflects incident radio frequency (RF) signals to transmit its information to the receiver. While backscattering technology was first used in Second World War to differentiate the allies’ and enemies’ aircraft, it was then used in commercial applications since the 1960s, especially in low-power and green communications¹ [2]. It forms the basis for the rapid growth of the Internet of Things (IoT), as it enables IoT devices to significantly reduce manufacturing and operating costs [3] and prolong their lifespan. A comprehensive survey on using BackCom-based green IoT for joint sensing and wireless

communication is presented in [4]. The survey describes the underlying operating principles, explores various applications, and identifies the associated challenges. Despite the promising applications of BackCom, the low efficiency of backscattering in far-field applications remains a major bottleneck [5]–[7]. Specifically, the utility of BackCom systems is limited by the energy that can be harnessed by the tag from the incident signals, which are used for transmitting information to the receiver. Therefore, novel backscattering modulation designs are needed to enhance the harvested power at the tags and satisfy the underlying BackCom information transmission requirements.

A. State-of-the-Art

In a BackCom system, the information transfer process involves an emitter broadcasting an RF signal that serves as a source of power for the passive backscatter tag². The tag leverages the RF signal for energy harvesting and signal backscattering, enabling it to transmit its information to the receiver upon interrogation [9]. The performance of a BackCom system is generally characterized by the data rate, tag-to-reader transmission range, power transmission, and bit error rate (BER) [10], [11]. The data rate is determined by a tag’s baseband bandwidth and the bits per symbol (bps) of the backscattered signal. The transmission range is dependent on the tag sensitivity, reader sensitivity, and BER. Understanding and optimizing these performance metrics is crucial for improving the efficiency and reliability of BackCom systems.

Unlike conventional wireless communication devices, backscatter tags do not have active RF components but exploit load modulation to transmit information. Specifically, the tag switches the load impedance at the antenna output terminal to modulate the backscattered signal with data [8], [12]. The selected load impedances depend on the designed modulation scheme. The 3 prominent modulation schemes being used in BackCom for data transmission are amplitude-shift keying (ASK), phase-shift keying (PSK), and frequency-shift keying (FSK) [13], [14].

The main advantage of using load modulation is that it offers low power consumption and a simple circuit design. However, the operation of the tag is strongly contingent on

²In general, there are 3 main types of backscatters tags, which are passive, semi-passive, and active tags [8]. The passive tag is a batteryless device that harvests energy from an external power source to support its circuit operation. In contrast, semi-passive and active tags are integrated with a battery. The semi-passive tag still utilizes the emitter’s RF carrier for signal backscattering, whereas the active tag can operate independently.

A. C. Y. Goay, D. Mishra, and A. Seneviratne are with the School of Electrical Engineering and Telecommunications, University of New South Wales, Sydney, NSW 2052, Australia (email: a.goay@student.unsw.edu.au, d.mishra@unsw.edu.au, a.seneviratne@unsw.edu.au).

A preliminary conference version of this work was presented at IEEE MASCOTS Workshop in Nice, France, in October 2022 [1].

¹Generally, the BackCom system can be classified based on the read range and system configuration. It can be divided into 2 segments: near-field and far-field BackCom systems. These segments differ significantly in terms of operating frequency band and hardware design. The near-field BackCom system utilizes magnetic coupling for information transfer and typically operates at 125 kHz or 13.56 MHz. In contrast, the far-field BackCom system operates in the 860 - 960 MHz frequency band and utilizes electromagnetic radiation for information transfer.

the selected load impedances. Since the tag performance is highly load-dependent [15], [16], existing research has revealed that load selection plays a significant role in the BackCom system. In [17], Nikitin *et al.* have shown that the maximum read range varies significantly with different load impedances and that the read range decreases exponentially with the mismatching degree. Another work demonstrated simple rules for load selection to achieve a long transmission range, with one load perfectly matched to the antenna impedance and another greatly mismatched [18]. Bletsas *et al.* [16] illustrated the load selection policy for minimizing BER for ASK and PSK modulations without considering tag power sensitivity. In contrast to [16]–[18], De Vita *et al.* [13] proposed a load impedance selection with an equal mismatch in both states. In [19], Karthaus *et al.* investigated the load impedance selections exploited in [13], [16], [17], and showed the harvested power varies with modulation depth.

With backscattering technology enabling low-cost and low-powered wireless communication, there is a growing interest in increasing the data rates of backscatter devices [20]. Concretely speaking, achieving a higher data rate with higher bits per symbol is preferable rather than increasing baseband frequency due to the high power usage. Recent works have explored high-order modulation techniques to increase the data rate. For instance, ambient BackCom systems employing M-ary PSK (*M*-PSK) and M-ary FSK (*M*-FSK) modulation scheme to enhance the data rate have been investigated [21], [22]. Additionally, the reflection coefficient selection for M-ary quadrature amplitude (QAM) modulation at the tag to achieve an equal Euclidean distance in the constellation diagram has been proposed [23]. A 4-QAM modulator designed for Radio Frequency Identification (RFID) tags is proposed in [24], with a focus on minimizing power loss while ensuring a minimum BER. Furthermore, prior works have explored spatial modulation in ambient BackCom systems, aiming to achieve both high data rates and spectrum efficiency [25], [26].

Furthermore, some research works have explored numerous methods of improving the BackCom system performance. For instance, the authors in [27] have investigated the use of bistatic architecture to maximize the tag-to-reader read range. The authors in [28] proposed a novel time-division multiple access protocol for the tag-to-tag cooperative scheme to enhance the throughput in a 3-tag BackCom system. Kimionis *et al.* [29] proposed utilizing reflection amplifiers to maximize the signal-to-noise ratio (SNR). Additionally, an unequal forward error correction coding technique is investigated to balance the trade-off between harvested power and BER in [30]. Apart from these methods, the backscatter tag's system throughput maximization by jointly optimizing the reflection coefficient is studied in [31].

B. Motivation and Contributions

The BackCom system performs poorly in far-field applications because the harvested energy at the tag decreases dramatically over longer distances [32]. Thus, the passive tag's transmission range is generally short and cannot exe-

cute advanced tasks. Therefore, the utility of the tag can be significantly improved by maximizing the harvested power at the tag. This will also enable the tag to perform more onboard tasks and support more applications. Additionally, our objective is to develop a high-data-rate BackCom system using the high-order M-ary ASK (*M*-ASK) modulation scheme. Unlike existing works that consider equal probability for the transmit symbols during backscattering, our investigation focuses on maximizing the average harvested power with unequal symbol probabilities.

Besides, the authors in [13], [16]–[19] have stated different load selections without finding the optimal value for enhancing the tag performance. *To the best of our knowledge, the tag's average harvested power maximization with optimal reflection coefficient selection for M-ASK modulation under the symbol error rate (SER), reader sensitivity, and energy constraints has not been investigated yet.* In this work, we conducted a comprehensive investigation and provided the closed-form global optimal solution to the tag's harvested power maximization problem. The unique features and contributions of this article are as follows:

- 1) We elaborate on the load-dependent performance metrics, including the harvested power, backscattered power, and SER. Then, we formulate a backscatter tag's harvested power maximization problem by jointly optimizing the reflection coefficients for the *M*-ASK modulation scheme while considering all of the operational requirements.
- 2) We leverage the non-trivial properties of the reflection coefficient in the ASK modulation to reduce the optimization variables of the original problem in half and transform it into a simplified equivalent form. This novel transformation helps obtain key analytical insights that will make obtaining the closed-form expression for the optimal backscattering coefficients possible.
- 3) We decouple the non-convex problem into 2 parts and solve it by transforming an inequality constraint into an equality constraint and reformulating the problem that is proved to be convex. Then, we solve the problem and obtain the global optimal solution by iteratively determining all the solution sets corresponding to different sequences of transmit symbols' probability.
- 4) We studied a particular case of tag design with binary ASK (BASK) modulation specifically for the applications in RFID under the EPC Class 1 Gen 2 protocol and developed a closed-form solution using the Karush-Kuhn-Tucker (KKT) conditions. This BASK modulation design, owing to its simplicity, suits for low-cost sensing and low-rate communication systems.
- 5) Simulation results are presented to quantify the maximum average harvested power for different applications under the varying value of the key system parameters. Here, we provided the design insight on the optimal reflection coefficients and verified the utility of the proposed optimal design.

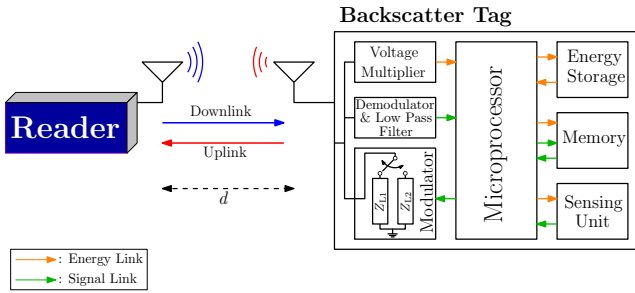


Fig. 1: Monostatic BackCom system model.

C. Paper Organization and Notations Used

This paper is organized as follows. Section II describes the BackCom system model and backscatter tag signal transmission with its modulation technique. In section III, the performance metrics of backscatter tags are discussed in more detail. Sections IV and V present the optimization problems and the solution methodology, respectively. The numerical results are shown in section VI, and a summary that concludes this work is provided in Section VII.

Notations: In this paper, $\text{Re}(\cdot)$ and $\text{Im}(\cdot)$ return the real part and imaginary part of a complex number, respectively. The upper-case boldface letters denote the matrix, and the lower letter of the matrix with the underscore of nm represents the matrix's (n, m) -th entry. The operator $\mathbb{E}[\cdot]$ denotes the average over the random variables in $[\cdot]$. Additionally, $|\cdot|$ returns the absolute value, and $j = \sqrt{-1}$ represents the imaginary unit.

II. SYSTEM DESCRIPTION

A. System Model and Transmission Protocol

This paper studies a monostatic BackCom system with one reader and one passive tag separated by distance d in a free-space transmission medium, as shown in Fig. 1. As a dedicated power source, the reader stably broadcasts an unmodulated RF carrier with constant power to the passive tag in the downlink. Then, the passive backscatter tag³, as an IoT device with sensing capability, transmits the backscattered signal that consists of a unique identifier and the sensing data to the reader in the uplink. As depicted in Fig.1, the passive tag comprises an antenna, voltage multiplier (VM), demodulator, low-pass filter (LPF), modulator, microprocessor, energy storage, memory, and a sensing unit⁴.

When a sinusoidal electromagnetic (EM) wave is impinging the tag antenna, the VM rectifies the induced voltage into DC power and delivers it to the microprocessor. Besides, the induced voltage is used to generate the low-frequency subcarrier, which is subsequently used to produce the modulated subcarrier with baseband signal [32]. Once the microprocessor is activated, the modulator will use the modulated

³There are various passive backscatter tags, of which the RFID tag is the most well-known one. In the latest research, the traditional RFID tag integrated with sensing electronics, transforming it into a sensing and computational platform, has been studied for IoT applications. The tag with sensing capability is called computational RFID (CRFID), which has higher power consumption during operation [3].

⁴A basic RFID tag comprises only a receiver antenna, modulator, VM, LPF, and an integrated circuit (IC) chip [32].

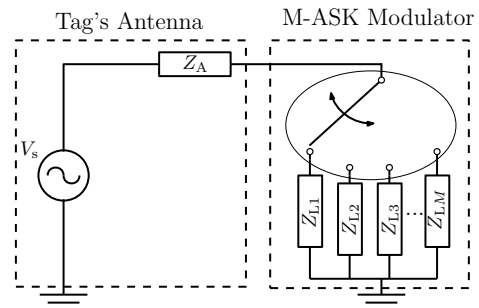


Fig. 2: Equivalent Thevenin Circuit of the Backscatter Tag with Minimum Scattering Antenna for M -ASK Modulation.

subcarrier to encode the backscattered signal by switching between different connection loads. These load impedances are selected depending on the system requirements and modulation scheme. In this paper, we focus on a BackCom system operating with the ASK modulation scheme. Our system model can be extended to accommodate multiple tags with minimal modifications by including a protocol for medium access control (MAC). In most BackCom systems, the ALOHA protocol is generally used as the MAC for anticollision [33], [34].

B. M -ary ASK Modulation

This section introduces the M -ASK modulation scheme for the backscatter tag. Specifically, $M = 2^n$ with $n \in \{1, 2, 3, 4, \dots\}$ represents the total number of bits in each transmit symbol. For example, the transmit symbols are $\{‘1’, ‘0’\}$ when $n = 1$, and $\{‘11’, ‘10’, ‘01’, ‘00’\}$ when $n = 2$. As the tag exploits load modulation, it will connect to different load impedances to transmit each symbol. Hence, there is M number of load impedances ($Z_{L1}, Z_{L2}, Z_{L3}, \dots, Z_{LM}$) that each represents a symbol ($S_1, S_2, S_3, \dots, S_M$) in the M -ASK modulator. An equivalent Thevenin circuit of the backscatter tag with the M -ASK modulator is illustrated in Fig.2. Without any loss of generality, we set the order of Z_{Li} to represent the symbol in the descending order of their decimal value. For example, in 4-ASK, the symbols $\{‘11’, ‘10’, ‘01’, ‘00’\}$ correspond to the underlying load impedances Z_{L1}, Z_{L2}, Z_{L3} and Z_{L4} , respectively.

III. PERFORMANCE METRICS FOR BACKSCATTERING

In [10], [11], authors presented the main factors that decide the maximum transmission range of the BackCom system are tag sensitivity, reader sensitivity, and SER. We consider these 3 system design factors and review them in the tag design.

A. Tag Power Sensitivity

Since the backscatter tag alters its circuit impedance to modulate the backscattered signal, the energy harvesting at the tag highly depends on the selected load impedance at each state. In general, the reflection coefficient is used to characterize the circuit impedance of the tag during backscattering. According to Kurokawa [35], the reflection coefficient is defined as the ratio of the reflected power wave to the total incident power wave. This paper denotes Γ_i

as the reflection coefficient, for $i \in \mathbb{M} = \{1, 2, 3, \dots, M\}$ represents when the tag connects to Z_{Li} and transmits symbol S_i . The Γ_i is given by [35]:

$$\Gamma_i \triangleq \frac{Z_{Li} - \bar{Z}_A}{Z_{Li} + Z_A}, \quad \forall i \in \mathbb{M}, \quad (1)$$

where $Z_A = R_A + jX_A$ is the antenna impedance, \bar{Z}_A is the conjugate of Z_A , and $Z_{Li} = R_{Li} + jX_{Li}$. The R_{Li} and R_A are the load resistance and antenna resistance, respectively, whereas X_{Li} and X_A are the load reactance and antenna reactance. To simplify the design optimization without the loss of generality, we substitute the expression of Z_A , \bar{Z}_A and Z_{Li} into (1) and express it in the rectangular form as below:

$$\begin{aligned} \Gamma_i &= \frac{R_{Li}^2 - R_A^2 + (X_{Li} + X_A)^2 + j2R_A(X_{Li} + X_A)}{(R_{Li} + R_A)^2 + (X_{Li} + X_A)^2} \\ &= \Gamma_{ai} + j\Gamma_{bi}, \quad \forall i \in \mathbb{M}, \end{aligned} \quad (2)$$

where $\Gamma_{ai} = \frac{R_{Li}^2 - R_A^2 + (X_{Li} + X_A)^2}{(R_{Li} + R_A)^2 + (X_{Li} + X_A)^2}$ and $\Gamma_{bi} = \frac{2R_A(X_{Li} + X_A)}{(R_{Li} + R_A)^2 + (X_{Li} + X_A)^2}$. The reflection coefficient is the key parameter determining the BackCom system's tag performance. Knowing that the tag can harvest energy and backscatter signal simultaneously, the power allocation in the tag during BackCom depends on Γ_i . Here, we define the harvested power P_{Li} as the power delivered to the microprocessor⁵, which is given by [12]:

$$\begin{aligned} P_{Li} &\triangleq \mathcal{E}_h P_a (1 - |\Gamma_i|^2) \\ &\stackrel{(s_1)}{=} \mathcal{E}_h P_a (1 - \Gamma_{ai}^2 - \Gamma_{bi}^2), \quad \forall i \in \mathbb{M}, \end{aligned} \quad (3)$$

where (s_1) is obtained using (2). The parameter $\mathcal{E}_h \in [0, 1]$ is the tag energy harvesting efficiency, and P_a is the maximum available power of P_{Li} . In this paper, we consider a general channel with a close-in free space reference distance model⁶ [38], [39], and hence P_a is given as:

$$P_a \triangleq P_t G_t G_r \left(\frac{\lambda}{4\pi d_o} \right)^2 \left(\frac{d_o}{d} \right)^n \quad (4)$$

where $d_o = 1\text{m}$ is the reference distance [40], P_t denotes the input power of the reader's antenna, G_t and G_r are the antenna gains of tag and reader, respectively, n is the path loss exponent, and $\lambda = \frac{c}{f}$ is the wavelength of the RF carrier with c as the speed of light and f is the carrier frequency.

In general, the passive backscatter tag's circuitry operation can be designed into 2 different models, which are instantaneous backscatter (continuous operation or non-duty-cycled

operation) and with harvest-then-transmit (HTT) protocol⁷ (duty-cycled operation) [42], [43]. The former design model enables the tag to harvest and power its circuitry directly during backscattering, while the latter requires an energy harvesting period. In particular, the HTT design model operates by consuming both the power from the incident EM wave and the onboard energy storage, which is charged during the energy harvesting period. The design selection of the tag is based on the operating environment, the tag's voltage and power requirements, and many more factors. The tag remains off and is only activated when sufficient power and a minimum threshold voltage are provided. During operation, the tag requires a minimum harvested power threshold, denoted as $P_{L,\min}$, for signal backscattering. Specifically, the tag relies on $P_{L,\min}$ to sustain its circuitry operation in instantaneous backscattering designs. In contrast, the tag that exploits HTT protocol uses the RF carrier to produce the clock signal [32], requiring the incident carrier with $P_{L,\min}$ to generate the baseband signal. In both design models, the tag is not activated, and no information will be generated when $P_{Li} < P_{L,\min}$. Hence, ensuring $P_{Li} \geq P_{L,\min}$ serves as the sustainability requirement of the BackCom system.

B. Reader Sensitivity

The second tag design consideration factor is reader sensitivity, which is the minimum required power $P_{r,\min}$ of a received signal where the reader can decode and retrieve the data in the given noise environment. It is noticed that in the BackCom system, the received signal at the reader is the backscattered signal of the tag after propagating through the transmission channel. Hence, the power of the received signal P_{ri} at the reader is proportional to the power of the backscattered signal P_{bi} at the tag. Since we consider the BackCom system with the free-space transmission, the power of the received signal at the reader is:

$$P_{ri} \triangleq P_{bi} G_r \left(\frac{\lambda}{4\pi d_o} \right)^2 \left(\frac{d_o}{d} \right)^n, \quad \forall i \in \mathbb{M}, \quad (5)$$

While many existing studies simplify their analysis by not considering structural mode scattering in the backscattered signal, we address this aspect in our work. Specifically, we account for the influence of structural mode scattering and assume the tag is equipped with a minimum scattering antenna⁸ [45]. Hence, P_{bi} is given by [46]:

$$\begin{aligned} P_{bi} &\triangleq \mathcal{E}_b P_a G_t |1 - \Gamma_i|^2 \\ &\stackrel{(s_2)}{=} \mathcal{E}_b P_a G_t \left[(1 - \Gamma_{ai})^2 + \Gamma_{bi}^2 \right], \quad \forall i \in \mathbb{M}, \end{aligned} \quad (6)$$

where (s_2) is obtained using (2) and $\mathcal{E}_b \in [0, 1]$ is the tag's backscattering efficiency. We see that P_{bi} is load-dependent,

⁵In reality, the energy harvesting model of UHF passive tags exhibits nonlinearity due to the nonlinear behavior of diodes in the voltage multiplier [13]. However, it is commonly observed that the actual nonlinear energy harvesting model can be effectively approximated by a linear model [36]. Consequently, the energy harvesting model employed in our study, which is widely adopted in most research, serves as a suitable approximation to the real model with minimal deviation.

⁶This model can be applied to the 0.5-100 GHz frequency band [37] and can be reduced to Friis transmission model (free space path loss) when we set $n = 2$.

⁷The WISP tag is a prime example of a passive backscatter tag operating on a duty cycle. With its additional sensing, computation, and data storage capabilities, the WISP tag requires higher power consumption compared to conventional passive RFID tags. Therefore, its operation adopts the duty cycle approach that switches between energy harvesting and backscattering. The operational power cycle is shown in [41].

⁸We have introduced a signal subtraction technique that ensures the practicality of the minimum scattering antenna assumption, thus allowing the optimal reflection coefficients determined based on this assumption applicable to all types of antennas without any performance degradation [44].

as it varies significantly with the selected Γ_i . Hence, the reader sensitivity of the BackCom system set a constraint in reflection coefficient selection at the tag. Since we focus on the tag design in this paper, $P_{bi} \geq P_{b,\min}$ served as one of the BackCom system operation requirements to satisfy the reader sensitivity.

C. Symbol Error Rate

The third factor limiting the tag performance is the SER, defined as the number of symbols misidentified by the reader over the total number of transmitted symbols at a given time interval [47]. The probability $P_e^{(i,k)}$ is the ratio of S_i being misidentified as S_k to the total number of transmitted S_i , which can be determined by the following equation [45]:

$$P_e^{(i,k)} \triangleq \frac{1}{2} \operatorname{erfc} \left(\frac{|V_0| m_{i,k}}{2\sqrt{2}\sigma} \right), \quad \forall i, k \in \mathbb{M}, i \neq k, \quad (7)$$

where $V_0 = \sqrt{8R_r P_{r,m}}$ is the induced voltage at the reader's antenna when the tag is scattering EM wave at the perfect matched condition ($Z_{Li} = \bar{Z}_A$) [19], where R_r representing the reader's antenna resistance and $P_{r,m} = \mathcal{E}_b P_a G_t G_r \left(\frac{\lambda}{4\pi d_o} \right)^2 \left(\frac{d_o}{d} \right)^n$. The inevitable additive white Gaussian noise n_r at the reader's antenna is assumed to have zero mean with $\mathbb{E}[|n_r|^2] = \sigma^2$. Besides, the modulation index $m_{i,k} \in [0, 1]$ is the characteristic difference between the two transmit symbols S_i and S_k , which is defined below [45]:

$$m_{i,k} \triangleq \frac{|\Gamma_i - \Gamma_k|}{2 \sqrt{(\Gamma_{ai} - \Gamma_{ak})^2 + (\Gamma_{bi} - \Gamma_{bk})^2}}, \quad (8)$$

$\forall i, k \in \mathbb{M}, i \neq k$, and (s_3) is obtained using (2). We set $\nu = \frac{|V_0| m_{i,k}}{2\sqrt{2}\sigma}$, and the complementary error function $\operatorname{erfc}(\nu) = 1 - \operatorname{erf}(\nu)$. Given that $\operatorname{erf}(\nu)$ is the error function, this implies the higher the $m_{i,k}$, the lower the SER. Concretely speaking, each transmitted symbol must exhibit unique characteristics to be distinguished from other symbols. This can be achieved by ensuring the modulation index of any 2 backscattered signals is greater than a threshold m_{th} . Therefore, we set a tag design requirement of $m_{i,k} \geq m_{\text{th}}$ to ensure that the SER remains within acceptable limits.

IV. PROBLEM DEFINITION

This section presents the problem formulation necessary to maximize the average harvested power at the passive tag under two distinct cases. In section IV-A, we consider the general case where the BackCom system operates with M -ASK modulation scheme and satisfies the underlying reader sensitivity, tag sensitivity, and SER requirements. We formulate an optimization problem to determine the optimal reflection coefficients, which deliver the maximum power to the tag while adhering to the operational constraints. In the second case, we formulate a new problem by considering BASK modulation scheme and relaxing the reader sensitivity constraint. Specifically, we assume that the backscattered

signal will always have sufficient power to be received by the reader. We will further discuss the details of this case in section IV-B.

A. Optimization Formulation in General Case

When activated, the tag arbitrarily backscatters the symbol S_i that carries $\log_2 M$ number of bits while delivering P_{Li} to the tag. We denote p_i as the occurrence probability of S_i , with $p_i \in [0, 1]$ and $\sum_{i=1}^M p_i = 1$. Besides, we set $\mathbf{p} = [p_1, p_2, \dots, p_M]$, and $p_i \geq p_{i+1}$ without any loss of generality. In general, it is not necessary that each transmit symbol has the same occurrence probability. Non-equiprobable signaling has been explored and can be advantageous [48], [49]. Hence, we consider p_i as application dependent constant, and the average harvested power $P_{L,\text{avg}}$ delivered to the tag is given by:

$$P_{L,\text{avg}} = \sum_{i=1}^M p_i P_{Li}, \quad (9)$$

The reason that motivates $P_{L,\text{avg}}$ maximization is to provide more power to the tag, which is essential in low-power and low-bandwidth applications such as backscatter-assisted IoT sensing and identification.⁹ The increase in $P_{L,\text{avg}}$ at the tag leads to greater harvested energy, which can be allocated to power additional sensing units, such as temperature sensors, humidity sensors, accelerometers, and cameras. This, in turn, allows for the collection of more data using the same resources for BackCom. Hence, maximizing $P_{L,\text{avg}}$ is essential for optimizing the efficiency of the IoT network.

Given $P_{L,\text{avg}}$ is a function of Γ_i , we are interested in determining the optimal reflection coefficients to maximize $P_{L,\text{avg}}$, subjecting to the following constraints. Constraint $C1$ defines the domain of the power reflection coefficient $|\Gamma_i| \leq 1$, whereas $C2$ and $C3$ include the boundary conditions for Γ_{ai} and Γ_{bi} , respectively. To meet the minimum SER requirement, the tag's modulation index $m_{i,k}$ must be greater than m_{th} , as stated in constraint $C4$. Furthermore, constraint $C5$ ensures the tag can continuously generate the information signal by setting the tag to at least harvest the minimum power threshold $P_{L,\min}$ at all states. Moreover, constraint $C6$ requires the backscattered signal of all different symbols to be greater than the minimum backscattered power threshold $P_{b,\min}$ to make sure the reader can accurately receive and decode the signal. Incorporating these constraints and setting maximizes $P_{L,\text{avg}}$ as the objective, the optimization problem is defined as:

$$\begin{aligned} (P1) : & \max_{\Gamma} P_{L,\text{avg}} \\ \text{s.t. } & C1 : \Gamma_{ai}^2 + \Gamma_{bi}^2 \leq 1, \quad \forall i \in \mathbb{M}, \\ & C2 : \Gamma_{ai} \in [-1, 1], \quad \forall i \in \mathbb{M}, \\ & C3 : \Gamma_{bi} \in [-1, 1], \quad \forall i \in \mathbb{M}, \end{aligned}$$

⁹For a tag operating with HTT protocol, the total energy consumed for circuitry operation during backscattering comprises both the energy harvested during the energy harvesting period and the backscattering period. Typically, an additional reflection coefficient is set to 0 during the harvesting period to maximize energy harvesting efficiency. Consequently, the duty cycle is shorter, enabling more data transmission when $P_{L,\text{avg}}$ is higher.

$$\begin{aligned}
C4 : & \frac{\sqrt{(\Gamma_{ai} - \Gamma_{ak})^2 + (\Gamma_{bi} - \Gamma_{bk})^2}}{2} \geq m_{th}, \\
& \forall i, k \in \mathbb{M}, i \neq k, \\
C5 : & \mathcal{E}_h P_a (1 - \Gamma_{ai}^2 - \Gamma_{bi}^2) \geq P_{L,\min}, \forall i \in \mathbb{M}, \\
C6 : & \mathcal{E}_b P_a G_r \left[(1 - \Gamma_{ai})^2 + \Gamma_{bi}^2 \right] \geq P_{b,\min}, \forall i \in \mathbb{M}.
\end{aligned}$$

where $\mathbf{\Gamma} = [\Gamma_{a1}, \Gamma_{b1}, \Gamma_{a2}, \Gamma_{b2}, \dots, \Gamma_{aM}, \Gamma_{bM}]$ are the optimization variables of problem (P1). By solving (P1), we obtain the maximum $P_{L,\text{avg}}$ (denoted as $P_{L,\text{avg}}^*$) by jointly optimizing $\mathbf{\Gamma}$. It should be noted that maximizing $P_{L,\text{avg}}$ implies the maximization of harvested energy when the reader interrogates the tag¹⁰. Since the passive tag only requires $P_{L,\min}$ to operate during backscattering, the surplus power is delivered to the energy storage system. The total stored energy $E_{\text{st}} = (P_{L,\text{avg}}^* - P_{L,\min})T$ over the interrogation period T is then used to sustain onboard operations during idle state.¹¹ Thus, the allowable onboard operations of the passive tag depend on $P_{L,\text{avg}}^*$.¹²

Problem (P1) maximizes $P_{L,\text{avg}}$ by determining the optimal $\mathbf{\Gamma}$ (denoted as $\mathbf{\Gamma}^*$), which implies (P1) is a $2M$ -variable optimization problem. We introduce the following Lemmas to transform problem (P1) into an M -variable problem to simplify the problem-solving process.

Lemma 1 *The average harvested power is maximized when either $\Gamma_{ai} = 0$ or $\Gamma_{bi} = 0$, $\forall i \in \mathbb{M}$.*

Proof *First, on setting Γ_{bi} as constant, we find that $\frac{\partial^2 P_{Li}}{\partial \Gamma_{ai}^2} = -2P_a$, which implies P_{Li} is a concave function in Γ_{ai} . Therefore, for a given Γ_{bi} , the optimal value of Γ_{ai} maximizing P_{Li} as obtained by solving $\frac{\partial P_{Li}}{\partial \Gamma_{ai}} = 0$ is $\Gamma_{ai} = 0$. Likewise, we set Γ_{ai} as a constant and we find that $\frac{\partial^2 P_{Li}}{\partial \Gamma_{bi}^2} = -2P_a$, which implies P_{Li} is also a concave function in Γ_{bi} . Similarly, for a given Γ_{ai} , the maximum harvested power as obtained by solving $\frac{\partial P_{Li}}{\partial \Gamma_{bi}} = 0$ is $\Gamma_{bi} = 0$. Hence, we proved Lemma 1.*

Lemma 2 *While having the same harvested power, a real reflection coefficient, that is $\text{Im}(\Gamma_i) = \Gamma_{bi} = 0$ ensures a better receiver sensitivity at the reader as compared to the purely imaginary reflection coefficient having $\text{Re}(\Gamma_i) = \Gamma_{ai} = 0$.*

Proof *Refer to Appendix A for the proof of Lemma 2.*

¹⁰In backscattered-assisted IoT networks with time-division multiple access protocol, only one IoT node is activated to backscatter information in response to the reader's interrogation. Meanwhile, the remaining tags operate in either sleep mode or energy harvesting mode.

¹¹The backscatter tag remains in an idle state and is activated when receiving the query command from the reader. This period, during which the reader queries the tag and the tag responds by backscattering its information, is known as the interrogation period.

¹²The WISP tag, a backscatter tag with sensing capabilities, has several onboard sensors and electronic components, along with the capability to connect with external sensors. These include a temperature sensor, an RF-powered camera, a microcontroller, an analog-to-digital converter, and potentially other types of sensors [41], [50].

Using Lemmas 1 and 2, we can reformulate the optimization problem (P1) into (P2) as defined below:

$$\begin{aligned}
(P2) : & \max_{\mathbf{\Gamma}_a} P_{L,\text{avg}} \\
\text{s.t. } & C2, C7 : \frac{|\Gamma_{ai} - \Gamma_{ak}|}{2} \geq m_{th}, \forall i, k \in \mathbb{M}, i \neq k, \\
& C8 : \mathcal{E}_h P_a (1 - \Gamma_{ai}^2) \geq P_{L,\min}, \forall i \in \mathbb{M}, \\
& C9 : \mathcal{E}_b P_a G_r (1 - \Gamma_{ai})^2 \geq P_{b,\min}, \forall i \in \mathbb{M},
\end{aligned}$$

where $\mathbf{\Gamma}_a = [\Gamma_{a1}, \Gamma_{a2}, \dots, \Gamma_{aM}]$, and (P2) is a M -variable problem. By solving problem (P2), we will obtain $P_{L,\text{avg}}^*$ along with the optimal $\mathbf{\Gamma}_a$ (denoted as $\mathbf{\Gamma}_a^*$).

B. Optimization with BASK Modulation

Here, we study the binary encoding scheme in the backscatter tag, so-called BASK modulation, which is the most popular scheme in the current industry standard - EPC Global Gen-2. The BASK modulation can also be written as 2-ASK, as we set $M = 2$. Hence, the transmit symbols contain only one bit, either '1' or '0'. As a result, the probability of these 2 symbols is p_1 and p_2 , with $p_1 + p_2 = 1$. The average harvested power of the tag in the BASK modulation is reformulated as:

$$\hat{P}_{L,\text{avg}} = p_1 P_{L1} + (1 - p_1) P_{L2} \quad (10)$$

Likewise, we aim to maximize $\hat{P}_{L,\text{avg}}$ by jointly optimizing $\hat{\mathbf{\Gamma}} = [\hat{\Gamma}_{a1}, \hat{\Gamma}_{b1}, \hat{\Gamma}_{a2}, \hat{\Gamma}_{b2}]$ under the same BackCom system operational requirements in problem (P1). In contrast, we only consider C1–C5 and assume C6 is always satisfied in BackCom systems. This assumption is valid because commercial readers typically exhibit good receive sensitivity, and RFID tags are commonly downlink-limited.¹³ Therefore, we can relax constraint C6. Consequently, the corresponding optimization problem is formulated as follows:

$$\begin{aligned}
(P3) : & \max_{\hat{\mathbf{\Gamma}}} \hat{P}_{L,\text{avg}} \\
\text{s.t. } & C1, C2, C3, C4, C5.
\end{aligned}$$

Likewise, we can apply Lemmas 1 and 2 to reduce the 4-variable problem (P3) into a 2-variable problem. Hence, we set $\Gamma_{b1} = \Gamma_{b2} = 0$. Without the loss of generality, we assume $\Gamma_{a1} \geq \Gamma_{a2}$ and problem (P3) is reformulated as:

$$\begin{aligned}
(P4) : & \max_{\Gamma_{a1}, \Gamma_{a2}} \hat{P}_{L,\text{avg}} \\
\text{s.t. } & C2, C10 : \frac{\Gamma_{a1} - \Gamma_{a2}}{2} \geq m_{th}, \\
& C11 : \mathcal{E}_h P_a (1 - \Gamma_{ai}^2) \geq P_{L,\min}, \forall i \in \{1, 2\}.
\end{aligned}$$

To distinguish the optimal results of different formulated problems, we denote the maximum average harvested power as $\hat{P}_{L,\text{avg}}^*$ determined with the optimal solution $\hat{\mathbf{\Gamma}}^* = [\hat{\Gamma}_{a1}^*, \hat{\Gamma}_{a2}^*]$ in problem (P4). Next, we analyze problems (P2) and (P4) to develop the problem-solving methods in section V.

¹³The commercial Impinj RFID reader has a receive sensitivity of -84 dBm [51]. Additionally, the reader-to-tag distance in a monostatic BackCom system is typically short, as the passive tag requires significant power transfer from the reader in the downlink. Consequently, the minimum backscattered power constraint is often less critical and can be relaxed in most applications compared to the more crucial tag sensitivity constraint.

V. SOLUTION METHODOLOGY

A. Problem Feasibility

Before solving problems (P2) and (P4), we will need to verify their feasibility with the given $P_{L,\min}$, $P_{b,\min}$ and m_{th} . This step is crucial to ensure the existence of an optimal set of reflection coefficients that satisfies all the operational requirements of the BackCom system. The following feasibility check applies to problem (P2) and can be extended to problem (P4) if we relax C9 as it does not have $P_{b,\min}$ constraint.

First, considering the unconstrained problem (P2), we notice that the $P_{L,\text{avg}}$ is maximized when $\Gamma_{ai} = 0$, $\forall i \in \mathbb{M}$. However, constraint C7 does not allow this to happen because it sets the separation between any two reflection coefficients $|\Gamma_{ai} - \Gamma_{ak}|$ must be greater than $2m_{\text{th}}$. Since the separation between any two reflection coefficients is different, the minimum separation is specified in the following Lemma.

Lemma 3 *The minimum separation between the reflection coefficients from the optimal solution set is $|\Gamma_{ai} - \Gamma_{ak}| = 2m_{\text{th}}$, which is determined by setting them to satisfy C7 at equality.*

Proof We first set a reflection coefficient at the perfect matched condition, denoted as $\hat{\Gamma}^{(0)} = 0$. Then, we set 2 different real reflection coefficients $\hat{\Gamma}^{(1)}$ and $\hat{\Gamma}^{(2)}$, and the modulation indices between these 2 reflection coefficients and $\hat{\Gamma}^{(0)}$ are $m_1 = \frac{|\hat{\Gamma}^{(1)} - \hat{\Gamma}^{(0)}|}{2}$ and $m_2 = \frac{|\hat{\Gamma}^{(2)} - \hat{\Gamma}^{(0)}|}{2}$, respectively. As we set $m_1 < m_2$, we obtain:

$$\left| \hat{\Gamma}^{(1)} \right| < \left| \hat{\Gamma}^{(2)} \right|. \quad (11)$$

Since we know, from (2), the harvested power is greater with a lower reflection coefficient magnitude under the same operating circumstance. Hence, $\hat{\Gamma}^{(1)}$ will give a greater harvested power as compare with $\hat{\Gamma}^{(2)}$. This indicates that the minimum separation between reflection coefficients must be the lowest to achieve greater $P_{L,\text{avg}}$. Since constraint C7 needs to be satisfied, the minimum separation between the optimal reflection coefficients will satisfy it at equality, such that $|\Gamma_{ai} - \Gamma_{ak}| = 2m_{\text{th}}$. Hence, we proved Lemma 3.

Lemma 3 yields a corollary as stated below:

Corollary 1 *The difference between the largest reflection coefficient Γ_L and smallest reflection coefficient Γ_S of Γ_a is $\Gamma_L - \Gamma_S = 2m_{\text{th}}(M - 1)$.*

Proof Using Lemma 3 and knowing Γ_{ai} is a real number, we can represent all Γ_{ai} , $\forall i \in \mathbb{M}$, on a number line with an equal gap of $2m_{\text{th}}$ for any two adjacent reflection coefficients. Since there is M number of reflection coefficients in the M -ASK modulated tag design, there are $(M - 1)$ gaps between the largest and smallest optimal reflection coefficients. Hence, $\Gamma_L - \Gamma_S = 2m_{\text{th}}(M - 1)$.

From constraints C8 and C9, we can determine the upper bound Γ_{ub} and lower bound Γ_{lb} of Γ_{ai} . By rearranging C8 and C9, we able to show Γ_{ai} lies in the following range,

respectively:

$$-\sqrt{1 - \frac{P_{L,\min}}{\mathcal{E}_h P_a}} \leq \Gamma_{a,i} \leq \sqrt{1 - \frac{P_{L,\min}}{\mathcal{E}_h P_a}}, \quad (12)$$

$$\Gamma_{a,i} \leq 1 - \sqrt{\frac{P_{b,\min}}{\mathcal{E}_b P_a G_r}}, \quad \Gamma_{a,i} \geq 1 + \sqrt{\frac{P_{b,\min}}{\mathcal{E}_b P_a G_r}}. \quad (13)$$

From (12) and (13) along with constraint C2, Γ_{ub} and Γ_{lb} are determined as:

$$\Gamma_{\text{ub}} = \min \left(\sqrt{1 - \frac{P_{L,\min}}{\mathcal{E}_h P_a}}, 1 - \sqrt{\frac{P_{b,\min}}{\mathcal{E}_b P_a G_r}} \right), \quad (14)$$

$$\Gamma_{\text{lb}} = -\sqrt{1 - \frac{P_{L,\min}}{\mathcal{E}_h P_a}}. \quad (15)$$

Subsequently, we form a condition with the defined Γ_{ub} and Γ_{lb} to verify problem (P2) has at least one possible solution set. The feasibility check condition is specified in Theorem 1.

Theorem 1 *With the selected order of M -ASK modulation scheme, the formulated problems are feasible if and only if $M \leq 1 + \frac{\Gamma_{\text{ub}} - \Gamma_{\text{lb}}}{2m_{\text{th}}}$.*

Proof Since we know $\Gamma_L - \Gamma_S$ is the range that covers all Γ_{ai} on a number line, and we have proved that the upper and lower boundaries for Γ_{ai} are respectively Γ_{ub} and Γ_{lb} , $\Gamma_L - \Gamma_S$ must fit within the boundary to ensure feasibility. Thus, we have the condition $\Gamma_L - \Gamma_S \leq \Gamma_{\text{ub}} - \Gamma_{\text{lb}}$. By substituting $\Gamma_L - \Gamma_S = 2m_{\text{th}}(M - 1)$ and rearranging, we will obtain $M \leq 1 + \frac{\Gamma_{\text{ub}} - \Gamma_{\text{lb}}}{2m_{\text{th}}}$.

Remark 1 *From Theorem 1, we know that $m_{\text{th}} \leq \frac{\Gamma_{\text{ub}} - \Gamma_{\text{lb}}}{2(M-1)}$, indicating that the highest value of m_{th} decreases with increasing M . Consequently, the minimum achievable SER decreases with M .*

B. Optimal Reflection Coefficients for BASK Modulation

We first solve the relatively simpler problem (P4) to get a basic idea of the optimal reflection coefficients selection before solving (P2). We start with invoking a key characteristic of problem (P4) using Lemma 4.

Lemma 4 *Problem (P4) is a convex problem.*

Proof Refer to Appendix B for the proof of Lemma 4.

Since (P4) is a convex problem, we can claim that the KKT point is the global optimal solution. Keeping constraint C2 implicit, the Lagrangian of (P4) can be written as:

$$\begin{aligned} \mathcal{L}_1 = & -p_1 \mathcal{E}_h P_a (1 - \Gamma_{a1}^2) - (1 - p_1) \mathcal{E}_h P_a (1 - \Gamma_{a2}^2) \\ & + \lambda_1 \left(m_{\text{th}} - \frac{\Gamma_{a1} - \Gamma_{a2}}{2} \right) + \lambda_2 \left(\Gamma_{a1}^2 - 1 + \frac{P_{L,\min}}{\mathcal{E}_h P_a} \right) \\ & + \lambda_3 \left(\Gamma_{a2}^2 - 1 + \frac{P_{L,\min}}{\mathcal{E}_h P_a} \right), \end{aligned} \quad (16)$$

where λ_1 represents the Lagrange multiplier associated with C10, and λ_2, λ_3 correspond to C11. The KKT point can be found by solving the following equations.

$$\frac{\partial \mathcal{L}_1}{\partial \Gamma_{a1}} = 2p_1 \mathcal{E}_h P_a \Gamma_{a1} - \frac{1}{2} \lambda_1 + 2\lambda_2 \Gamma_{a1} = 0, \quad (17)$$

$$\frac{\partial \mathcal{L}_1}{\partial \Gamma_{a2}} = 2(1-p_1) \mathcal{E}_h P_a \Gamma_{a2} + \frac{1}{2} \lambda_1 + 2\lambda_3 \Gamma_{a2} = 0, \quad (18)$$

$$\lambda_1 \left(m_{\text{th}} - \frac{\Gamma_{a1} - \Gamma_{a2}}{2} \right) = 0, \quad (19)$$

$$\lambda_2 \left(\Gamma_{a1}^2 - 1 + \frac{P_{L,\min}}{\mathcal{E}_h P_a} \right) = 0, \quad (20)$$

$$\lambda_3 \left(\Gamma_{a2}^2 - 1 + \frac{P_{L,\min}}{\mathcal{E}_h P_a} \right) = 0. \quad (21)$$

along with $\lambda_1, \lambda_2, \lambda_3 \geq 0$. Equations (17) and (18) are the sub-gradient conditions, and (19),(20),(21) are the complementary slackness conditions. While solving (17) – (21), we obtain $\hat{\Gamma}^*$ in terms of the constant parameters, and thereby determine $\hat{P}_{L,\text{avg}}^*$. Next, we discuss the method to determine the underlying KKT point $(\hat{\Gamma}^*, \lambda_1^*, \lambda_2^*, \lambda_3^*)$ in Lemma 5.

Lemma 5 *The $\hat{\Gamma}^*$ is obtained from one of the 3 cases, which are case (a) : $\lambda_1 \neq 0, \lambda_2 = \lambda_3 = 0$, case (b) : $\lambda_1 \neq 0, \lambda_2 \neq 0, \lambda_3 = 0$, and case (c) : $\lambda_1 \neq 0, \lambda_3 \neq 0, \lambda_2 = 0$.*

Proof *First, we check whether λ_1 can be zero or not. Since the objective function is decreasing with Γ_{a1} and Γ_{a2} , the optimal solution without the constraints will have $\Gamma_{a1} = \Gamma_{a2} = 0$. However, constraint C10 requires a minimum separation between Γ_{a1} and Γ_{a2} . Therefore, as proved, constraint C10 is satisfied at equality, which implies λ_1 is always positive.*

It is noticed that λ_2 and λ_3 simultaneously greater than zero is very unlikely because this is feasible only when $m_{\text{th}} = \sqrt{1 - \frac{P_{L,\min}}{\mathcal{E}_h P_a}}$. When this condition holds, $\hat{\Gamma}^$ can be obtained from either case (b) or case (c). Therefore, the optimal solution is given by either or both λ_2 and λ_3 are zero, while $\lambda_1 > 0$.*

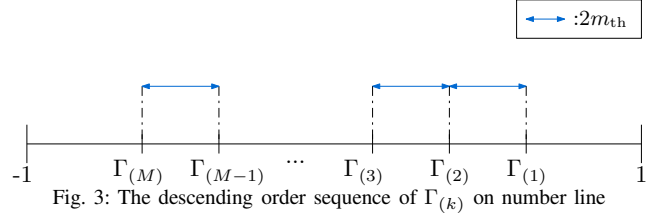
Thus, 3 different Γ_{a1} can be obtained from the 3 cases stated in Lemma 5, in which we denote Γ_{a1} obtained from case (a), (b) and (c) as $\hat{\Gamma}_{a1}^{(a)}$, $\hat{\Gamma}_{a1}^{(b)}$, and $\hat{\Gamma}_{a1}^{(c)}$, respectively. In case (a) where $\lambda_2 = \lambda_3 = 0$, $\hat{\Gamma}_{a1}^{(a)}$ is obtained with (17), (18) and (19). On the other hand, in case (b) where $\lambda_3 = 0$, $\hat{\Gamma}_{a1}^{(b)}$ is obtained with (20). Likewise, we use (19) and (21) to obtain $\hat{\Gamma}_{a1}^{(c)}$ in case (c) where $\lambda_2 = 0$. As a result, the closed-form expression of the solutions are:

$$\hat{\Gamma}_{a1}^{(a)} = 2(1-p_1) m_{\text{th}}, \quad (22a)$$

$$\hat{\Gamma}_{a1}^{(b)} = \sqrt{1 - \frac{P_{L,\min}}{\mathcal{E}_h P_a}}, \quad (22b)$$

$$\hat{\Gamma}_{a1}^{(c)} = -\sqrt{1 - \frac{P_{L,\min}}{\mathcal{E}_h P_a}} + 2m_{\text{th}}. \quad (22c)$$

From Lemma 4, we recall that problem (P4) is convex. Therefore, only one KKT point will satisfy all the constraints, which implies $\hat{\Gamma}_{a1}^*$ is selected from $\hat{\Gamma}_{a1}^{(a)}$, $\hat{\Gamma}_{a1}^{(b)}$ and $\hat{\Gamma}_{a1}^{(c)}$. Notably, all the optimal Lagrange multipliers $(\lambda_1^*, \lambda_2^*, \lambda_3^*)$ of the KKT point must be positive for it to be the optimal solution. It is noticed that λ_2 from case (b) is positive only when $\hat{\Gamma}_{a1}^{(b)} < \hat{\Gamma}_{a1}^{(a)}$, whereas λ_3 from case (c) is positive only when $\hat{\Gamma}_{a1}^{(c)} > \hat{\Gamma}_{a1}^{(a)}$. Besides, from (14), (15)



and Lemma 3, we notice that the range of $\hat{\Gamma}_{a1}^*$ is given as $[\hat{\Gamma}_{a1}^{(c)}, \hat{\Gamma}_{a1}^{(b)}]$. Hence, incorporating all these properties, $\hat{\Gamma}_{a1}^*$ is determined by:

$$\hat{\Gamma}_{a1}^* = \max \left\{ \hat{\Gamma}_{a1}^{(c)}, \min \left\{ \hat{\Gamma}_{a1}^{(a)}, \hat{\Gamma}_{a1}^{(b)} \right\} \right\}, \quad (23)$$

and $\hat{\Gamma}_{a2}^*$ is then determined by:

$$\hat{\Gamma}_{a2}^* = \hat{\Gamma}_{a1}^* - 2m_{\text{th}}. \quad (24)$$

Eventually, the maximum average harvested power that is determined from problem (P4) is:

$$\hat{P}_{L,\text{avg}}^* = \mathcal{E}_h P_a \left[p_1 \left(1 - \left(\hat{\Gamma}_{a1}^* \right)^2 \right) + p_2 \left(1 - \left(\hat{\Gamma}_{a2}^* \right)^2 \right) \right]. \quad (25)$$

Remarkably, we obtain the closed-form expression for the global solution of problem (P4). This signifies the utility of using KKT conditions to solve our optimization problem. From (22), (23), and (25), it is evident that the occurrence probabilities p_1 and p_2 are crucial factors. The maximum average harvested power in the unequal symbol probability scenario is clearly greater than in the equal symbol probability scenario, as illustrated graphically in Sec. VI.

Remark 2 *In the context of this case, it is observed that $\hat{\Gamma}_{ai}^*$ is closely linked to p_i . In particular, $\hat{\Gamma}_{ai}^*$ will be set closer to zero when p_i is higher. This highlights the significance of p_i in determining $\hat{\Gamma}_{ai}^*$. The implications of this observation can contribute to a better understanding of the underlying system and inform the development of more efficient and effective strategies for optimization.*

C. Optimal Reflection Coefficients for General Case

Here, we propose a method to solve problem (P2) and obtain the optimal reflection coefficients for the tag with M -ASK modulation in the general case. It is evident that (P2) is a non-convex problem as constraints C7 and C9 are non-convex. Therefore, we cannot obtain the global solution by applying the KKT conditions unless we transform it into a convex problem. Next, we will show how the original complex problem (P2) can be solved in 2 steps. Specifically, we first transform the original problem (P2) into a new convex problem under an assumption that will allow us to obtain a candidate of the global solution with the KKT conditions. Later, we determine all the candidates where the optimal solution is the solution set that gives the maximum $P_{L,\text{avg}}$. The details of these 2 steps are discussed in the following paragraphs.

Following Lemma 3, we can sequence elements of Γ_a on a number line, with the gap between any 2 adjacent reflection coefficients being $2m_{\text{th}}$. Although we still do not know the sequence of all Γ_{ai}^* , this characteristic will hold when we locate them on a number line. In this context, we denote $\Gamma_{(k)}$, $\forall k \in \mathbb{M}$ to represent the placement of all Γ_{ai} in descending order as shown in Fig. 3. Further, we set $p_{(k)}$ as the probability corresponding to $\Gamma_{(k)}$, and $\mathbf{p}_2 = [p_{(1)}, p_{(2)}, \dots, p_{(M)}]$. This implies the sequence of all Γ_{ai} can be determined with the corresponding p_i if all $p_{(k)}$ are known.

Assuming the sequence of all Γ_{ai}^* is known, which indicates $p_{(k)}$ is also known, we can use $\Gamma_{(k)}$, $\forall k \in \mathbb{M}$ as the optimization variables to determine $P_{L,\text{avg}}^*$. This assumption will be further validated by a proposed approach discussed later in the same section. With this assumption, we transform problem (P2) into problem (P5), where constraint C7 can be equivalently replaced by C12, which ensures the gap between any 2 adjacent $\Gamma_{(k)}$ is $2m_{\text{th}}$. Besides, as stated earlier, constraints C2, C8, and C9 provide the upper bound Γ_{ub} and lower bound Γ_{lb} for Γ_{ai} , which we can combine all these 3 constraints and form a new constraint C13 as $\Gamma_{\text{lb}} \leq \Gamma_{(k)} \leq \Gamma_{\text{ub}}$. Hence, under the assumption of $p_{(k)}$ is known, problem (P2) is equivalent to:

$$(P5) : \max_{\Gamma_{(a)}} P_{L,\text{avg}} = \sum_{k=1}^M p_{(k)} \mathcal{E}_h P_a \left(1 - \Gamma_{(k)}^2\right)$$

$$\text{s.t. } C12 : \Gamma_{(k)} = \Gamma_{(1)} - 2m_{\text{th}}(k-1), \quad \forall k \in \mathbb{M},$$

$$C13 : \Gamma_{\text{lb}} \leq \Gamma_{(k)} \leq \Gamma_{\text{ub}}, \quad \forall k \in \mathbb{M},$$

where $\Gamma_{(a)} = [\Gamma_{(1)}, \Gamma_{(2)}, \dots, \Gamma_{(M)}]$. Notice that C12 is an equality constraint, we substitute it into the objective function and turn it into a single-variable function of $\Gamma_{(1)}$, as follows:

$$P_{L,\text{avg}} = \mathcal{E}_h P_a \left[1 - \sum_{k=1}^M p_{(k)} \left(\Gamma_{(1)} - 2m_{\text{th}}(k-1)\right)^2\right] \quad (26)$$

Additionally, since we know $\Gamma_{(k)} > \Gamma_{(k+1)}$, constraint C13 will always satisfy when we set $\Gamma_{(1)} \leq \Gamma_{\text{ub}}$ and $\Gamma_{(M)} \geq \Gamma_{\text{lb}}$. Consequently, problem (P5) can be further transformed into a single variable problem as follows:

$$(P6) : \max_{\Gamma_{(1)}} P_{L,\text{avg}}$$

$$\text{s.t. } C14 : \Gamma_{(1)} - 2m_{\text{th}}(M-1) \geq \Gamma_{\text{lb}},$$

$$C15 : \Gamma_{(1)} \leq \Gamma_{\text{ub}},$$

where C14 and C15 are the boundary conditions of $\Gamma_{(1)}$. Next, Lemma 6 discusses the convexity of problem (P6).

Lemma 6 *Problem (P6) is a convex problem.*

Proof *Firstly, we determine the second derivative of the objective function, which is $\frac{\partial^2 P_{L,\text{avg}}}{\partial \Gamma_{(1)}^2} = -2\mathcal{E}_h P_a \sum_{k=1}^M p_{(k)}$.*

Clearly, $\frac{\partial^2 P_{L,\text{avg}}}{\partial \Gamma_{(1)}^2} < 0$, which implies the objective function of problem (P6) is concave. Moreover, the subjected constraints C14 and C15 are linear. Hence, problem (P6) is a convex optimization problem.

We can apply the KKT conditions to obtain the global solution for problem (P6) because it is a convex problem. Hence, the Lagrangian of problem (P6) is:

$$\mathcal{L}_2 = - \left[\mathcal{E}_h P_a - \mathcal{E}_h P_a \sum_{k=1}^M p_{(k)} \left(\Gamma_{(1)} - 2m_{\text{th}}(k-1)\right)^2 \right]$$

$$+ \lambda_4 \left(\Gamma_{\text{lb}} - \Gamma_{(1)} + 2m_{\text{th}}(M-1)\right)$$

$$+ \lambda_5 \left(\Gamma_{(1)} - \Gamma_{\text{ub}}\right), \quad (27)$$

where λ_4 and λ_5 are the Lagrange multipliers associated with C14 and C15, respectively. The KKT point $(\Gamma_{(1)}^*, \lambda_4^*, \lambda_5^*)$ that gives $P_{L,\text{avg}}^*$ is obtained by solving the following equations.

$$\frac{\partial \mathcal{L}_2}{\partial \Gamma_{(1)}} = 2\mathcal{E}_h P_a \sum_{k=1}^M p_{(k)} \left[\Gamma_{(1)} - 2m_{\text{th}}(k-1)\right]$$

$$- \lambda_4 + \lambda_5 = 0, \quad (28)$$

$$\lambda_4 \left(\Gamma_{\text{lb}} - \Gamma_{(1)} + 2m_{\text{th}}(M-1)\right) = 0, \quad (29)$$

$$\lambda_5 \left(\Gamma_{(1)} - \Gamma_{\text{ub}}\right) = 0. \quad (30)$$

along with $\lambda_4, \lambda_5 \geq 0$. Likewise, (28) is the sub-gradient condition, and (29) and (30) are the complementary slackness conditions. The method we use to determine the KKT point is stated in the following Lemma.

Lemma 7 *The $\Gamma_{(1)}^*$ is obtained from one of the 3 cases, which are case (a): $\lambda_4 = \lambda_5 = 0$, case (b): $\lambda_4 = 0, \lambda_5 \neq 0$, and case (c): $\lambda_4 \neq 0, \lambda_5 = 0$.*

Proof *Generally, the KKT point is determined by setting either or both λ_4 and λ_5 as either zero or non-zero values. In our problem, we noted that $\lambda_4 \neq 0$ and $\lambda_5 \neq 0$ only occur when $\Gamma_{\text{ub}} = \Gamma_{\text{lb}} + 2m_{\text{th}}(M-1)$. When this condition holds, the solution obtained from this case is the same as we obtained from either case (b) or case (c). Therefore, there are only 3 cases to be considered.*

We denote $\Gamma_{(1)}^{(a)}, \Gamma_{(1)}^{(b)}$, and $\Gamma_{(1)}^{(c)}$ as the solutions obtained from the 3 cases stated in Lemma 7. Specifically, in case (a), $\Gamma_{(1)}^{(a)}$ is obtained with (28). Likewise, $\Gamma_{(1)}^{(b)}$ in case (b) is obtained with (29), whereas $\Gamma_{(1)}^{(c)}$ in case (c) is obtained with (30). Subsequently, the closed-form expression for the solutions are:

$$\Gamma_{(1)}^{(a)} = 2m_{\text{th}} \sum_{k=1}^M p_{(k)} (k-1), \quad (31a)$$

$$\Gamma_{(1)}^{(b)} = \Gamma_{\text{ub}}, \quad (31b)$$

$$\Gamma_{(1)}^{(c)} = \Gamma_{\text{lb}} + 2m_{\text{th}}(M-1). \quad (31c)$$

Similarly, since (P6) is a convex problem, only one KKT point with $\lambda_4^*, \lambda_5^* \geq 0$ will satisfy all the constraints, which is selected from $\{\Gamma_{(1)}^{(a)}, \Gamma_{(1)}^{(b)}, \Gamma_{(1)}^{(c)}\}$. Specifically, we notice that λ_5 from case (b) is positive when $\Gamma_{(1)}^{(b)} < \Gamma_{(1)}^{(a)}$. In contrast, λ_4 from the case (c) is positive when $\Gamma_{(1)}^{(c)} > \Gamma_{(1)}^{(a)}$. Hence,

$\Gamma_{(1)}^*$ is determined by:

$$\Gamma_{(1)}^* = \max \left\{ \Gamma_{(1)}^{(c)}, \min \left\{ \Gamma_{(1)}^{(a)}, \Gamma_{(1)}^{(b)} \right\} \right\}, \quad (32)$$

Knowing the sequence of $\Gamma_{(k)}^*$ is a descending order with k on a number line, and therefore:

$$\Gamma_{(k+1)}^* = \Gamma_{(k)}^* - 2m_{\text{th}}, \quad \forall k \in \mathbb{M} \setminus M. \quad (33)$$

Subsequently, $P_{(L,\text{avg})}^*$ is determined by:

$$P_{(L,\text{avg})}^* = \mathcal{E}_h P_a \sum_{i=1}^M p_{(i)} \left(1 - \left(\Gamma_{(i)}^* \right)^2 \right). \quad (34)$$

Till this step, we solved problem (P6) and were able to obtain the closed-form expression for the global solution with the given of $p_{(k)}$, $\forall k$. However, we do not know the sequence of all Γ_{ai}^* , which means \mathbf{p}_2 is unknown. One possible solution to determine \mathbf{p}_2 is to consider all permutation sequences of \mathbf{p} . Using this approach, we should note that there is a maximum of $M!$ possible sequences, each of which can yield a candidate for Γ_a^* .

Considering all the permutation sequences of the symbols' probability for finding the candidate of Γ_a^* would require considerable computing time, especially when M is large. Nevertheless, from the solving process in Section V-B, we observe a regular pattern of $\hat{\Gamma}_{ai}^*$, which inspires an approach to simplify the calculation due to the $M!$ possible sequences of \mathbf{p} . Specifically, we note that symbols with higher occurrence probabilities have lower mismatch degrees. Consequently, the optimal reflection coefficient corresponding to higher occurrence probability will be set closer to 0 compared to those with lower occurrence probabilities. This implies Γ_{ai}^* is dominated by the symbol probability. Hence, the optimal solution of (P2) will satisfy the relationship $|\Gamma_{ai}^*| \leq |\Gamma_{ak}^*|$ for $p_i \geq p_k$, $\forall i, k \in \mathbb{M}$ and $i \neq k$.

In this context, once we locate Γ_{a1} , the remaining Γ_{ai} will be placed alternatively on both sides of Γ_{a1} . However, it might happen that either the left or right side is truncated due to the lower or upper bound constraint, and the remaining Γ_{ai} will then be placed sequentially on the other side. This approach significantly reduces the number of candidate solutions from $M!$ to $2(M-1)$. An example of this idea for 4-ASK is provided in the following matrix:

$$\begin{bmatrix} \Gamma_{a1} & \Gamma_{a2} & \Gamma_{a3} & \Gamma_{a4} \\ \Gamma_{a3} & \Gamma_{a1} & \Gamma_{a2} & \Gamma_{a4} \\ \Gamma_{a2} & \Gamma_{a1} & \Gamma_{a3} & \Gamma_{a4} \\ \Gamma_{a4} & \Gamma_{a3} & \Gamma_{a1} & \Gamma_{a2} \\ \Gamma_{a4} & \Gamma_{a2} & \Gamma_{a1} & \Gamma_{a3} \\ \Gamma_{a4} & \Gamma_{a3} & \Gamma_{a2} & \Gamma_{a1} \end{bmatrix} \iff \begin{bmatrix} p_1 & p_2 & p_3 & p_4 \\ p_3 & p_1 & p_2 & p_4 \\ p_2 & p_1 & p_3 & p_4 \\ p_4 & p_3 & p_1 & p_2 \\ p_4 & p_2 & p_1 & p_3 \\ p_4 & p_3 & p_2 & p_1 \end{bmatrix}$$

where the 6 rows in the left matrix are all the possible sequences of $[\Gamma_{a1}, \Gamma_{a2}, \Gamma_{a3}, \Gamma_{a4}]$ with the corresponding matrix of probabilities $[p_1, p_2, p_3, p_4]$ on the right. Therefore, we will only use the probability sequences from the above matrix to obtain $P_{L,\text{avg}}^*$ for the 4-ASK modulation scheme. A similar concept can be extended to M -ASK, where the method to obtain the probability sequences matrix is given in Algorithm 1.

Algorithm 1 provides us with matrix \mathbf{A} , and from there,

Algorithm 1 Generation of Sequence Matrix \mathbf{A}

Input: M, \mathbf{p}

Output: \mathbf{A}

```

1:  $N = 2(M - 1)$ 
2: Set  $\mathbf{A}^{N \times M} = \begin{bmatrix} a_{11} & a_{12} & \cdots & a_{1M} \\ a_{21} & a_{22} & \cdots & a_{2M} \\ \vdots & \vdots & \vdots & \vdots \\ a_{N1} & a_{N2} & \cdots & a_{NM} \end{bmatrix}$ 
3: for  $\omega_1 = 1$  to  $M$  do
4:    $a = \omega_1$ 
5:   for  $\omega_2 = 1$  to  $2$  do
6:      $\beta = 0$ 
7:     if  $\omega_1 \neq 1$  or  $\omega_2 \neq 1$  then
8:       if  $\omega_1 \neq M$  or  $\omega_2 \neq 2$  then
9:         for  $\omega_3 = 1$  to  $M$  do
10:          if  $\omega_2 = 1$  then
11:             $a \leftarrow a + (-1)^{\omega_3+1}(\omega_3 - 1)$ 
12:          else if  $\omega_2 = 2$  then
13:             $a \leftarrow a + (-1)^{\omega_3}(\omega_3 - 1)$ 
14:           $n = 2\omega_1 - (\frac{1}{2} + \frac{1}{2}(-1)^{\omega_2+1}) - 1$ 
15:          if  $a \leq M$  and  $a \geq 1$  and  $\beta = 0$  then
16:             $m = a$ 
17:          else
18:            if  $\omega_1 \leq \frac{M}{2}$  then
19:               $\beta = \omega_3$ 
20:            else
21:               $\beta = M - \omega_3 + 1$ 
22:             $m = \beta$ 
23:             $a_{nm} = p_{\omega_3}$ 
24: Return  $\mathbf{A}$ 

```

we use each row of \mathbf{A} as \mathbf{p}_2 to obtain all the candidate solutions with (32). During this process, we make use of the variable \mathbb{T} and matrix \mathbf{B} , to keep track of $P_{L,\text{avg}}^*$ and the corresponding $p_{(k)}$ and $\Gamma_{(k)}^*$, $\forall k \in \mathbb{M}$. As we iterate through each probability sequence in \mathbf{A} , we update \mathbb{T} and \mathbf{B} whenever $P_{L,\text{avg}}^*$ is greater than the current \mathbb{T} . This process continues until all probability sequences in \mathbf{A} have been used, and we will obtain the optimal \mathbf{p}_2 and $\Gamma_{(a)}$ that yields $P_{L,\text{avg}}^*$. Given that \mathbf{p}_2 represents one of the rows in matrix \mathbf{A} , and p_i in \mathbf{p} is arranged in descending order, we can obtain Γ_{ai}^* from $\Gamma_{(a)}$ by rearranging $\Gamma_{(k)}$ in $\Gamma_{(a)}$ such that the corresponding $p_{(k)}$ in \mathbf{p}_2 are arranged in descending order. By doing so, we can determine the global solution Γ_a^* of problem (P2) and $P_{L,\text{avg}}^*$. These steps are summarized in Algorithm 2. The $\text{sort}(\mathbf{E}, x)$ function, in Algorithm 2, sorts the columns of the input matrix \mathbf{E} in descending order based on the elements of the x row.

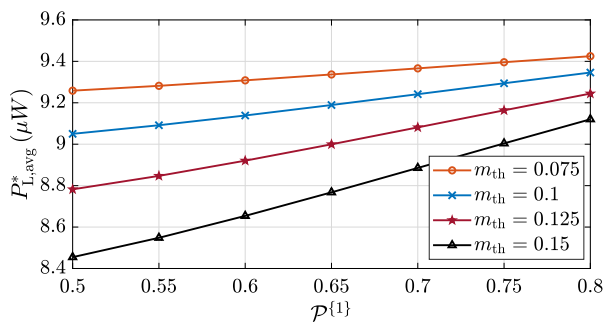
VI. RESULTS AND DISCUSSION

We numerically demonstrate the tag performance with our proposed optimal reflection coefficients. Specifically, we determine and observe the achievable $P_{L,\text{avg}}^*$ for different tag design parameters and BackCom systems. Unless otherwise stated, we set $P_t = 1\text{W}$, $f = 915\text{MHz}$, $c = 3 \times 10^8\text{ms}^{-1}$, $G_t = 4$, $G_r = 1.5$, $d_o = 1\text{m}$, $d = 7\text{m}$, $P_{L,\text{min}} = 5\mu\text{W}$, $P_{b,\text{min}} = 3\mu\text{W}$, $\mathcal{E}_h = \mathcal{E}_b = 0.8$, $\sigma^2 = -90\text{dBm}$ and

Algorithm 2 Optimal Reflection Coefficient for M -ASK Modulation

Input: M , m_{th} , $P_{L,min}$, $P_{b,min}$, P_t , G_t , G_r , d , f , n , \mathcal{E}_h and \mathcal{E}_b
Output: $\Gamma_{\mathbf{a}}$, $P_{L,avg}^*$

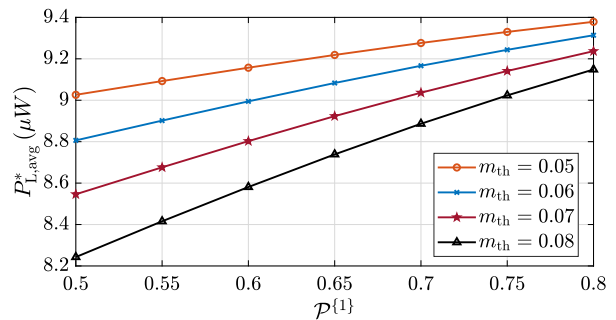
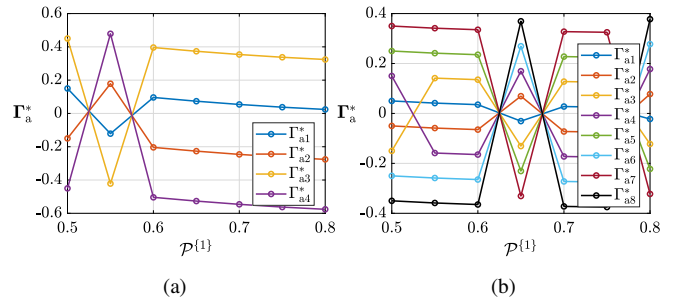
- 1: Run Algorithm 1 to obtain \mathbf{A}
 - 2: Set $\mathbb{T} = 0$
 - 3: **for** $\nu = 1$ to $2(M - 1)$ **do**
 - 4: **for** $u = 1$ to M **do**
 - 5: $p(u) = a_{\nu u}$
 - 6: $\Gamma_{(1)}^* = \max\left\{\Gamma_{(1)}^{(c)}, \min\left\{\Gamma_{(1)}^{(a)}, \Gamma_{(1)}^{(b)}\right\}\right\}$
 - 7: **for** $w = 1$ to M **do**
 - 8: $\Gamma_{(w)}^* = \Gamma_{(1)}^* - 2m_{th}(w - 1)$
 - 9: $P_{(L,avg)}^* = \mathcal{E}_h P_a \sum_{k=1}^M p(k) \left(1 - \left(\Gamma_{(k)}^*\right)^2\right)$
 - 10: **if** $P_{(L,avg)}^* > \mathbb{T}$ **then**
 - 11: $\mathbb{T} = P_{(L,avg)}^*$
 - 12: $\mathbf{B}^{2 \times M} = \begin{bmatrix} p(1) & p(2) & \dots & p(M) \\ \Gamma_{(1)}^* & \Gamma_{(2)}^* & \dots & \Gamma_{(M)}^* \end{bmatrix}$
 - 13: $\mathbf{C}^{2 \times M} = \text{sort}(\mathbf{B}, 1)$
 - 14: **for** $i = 1$ to M **do**
 - 15: $\Gamma_{ai}^* = c_{2i}$
 - 16: **Return** $\Gamma_{\mathbf{a}} = [\Gamma_{a1}^*, \Gamma_{a2}^*, \dots, \Gamma_{aM}^*]$, $P_{L,avg}^* = \mathbb{T}$
-


 Fig. 4: Design insights on $P_{L,avg}^*$ for 4-ASK.

$R_r = 50\Omega$. Besides, we consider our system model operates in shadowed urban areas, where the path loss exponent is set to $n = 3$ [52]. Depending on the modulation order M , each symbol's total number of bits will be $\log_2 M$. A sequence of bits '1' and '0' with the probability $\mathcal{P}^{\{1\}}$ and $\mathcal{P}^{\{0\}}$, respectively are used to generate the symbols. For example, considering 4-ASK, the transmit symbols are '11', '10', '01', and '00'. The corresponding symbol probabilities are $p_1 = (\mathcal{P}^{\{1\}})^2$, $p_2 = \mathcal{P}^{\{1\}}\mathcal{P}^{\{0\}}$, $p_3 = \mathcal{P}^{\{0\}}\mathcal{P}^{\{1\}}$, and $p_4 = (\mathcal{P}^{\{0\}})^2$. Without the loss of generality, we set $\mathcal{P}^{\{1\}} \geq \mathcal{P}^{\{0\}}$ to simplify our numerical investigation, which can be easily switched to fit the opposite case.

A. Insight on Optimal Reflection Coefficients

In practical scenarios, the sensor data and the unique identifier of the tag may exhibit a significant bias towards either bit '1' or '0'. We use this uneven occurrence probability of symbol to maximize the tag's harvested power since it is highly dependent on the reflection coefficient,


 Fig. 5: Design insights on $P_{L,avg}^*$ for 8-ASK.

 Fig. 6: Γ_{ai}^* versus $\mathcal{P}^{\{1\}}$ at $d = 7\text{m}$ with (a) 4-ASK, $m_{th} = 0.15$ and (b) 8-ASK, $m_{th} = 0.05$.

which is linked to the transmit symbols. We determine the correlation between $P_{L,avg}^*$ and $\mathcal{P}^{\{1\}}$ at different m_{th} for 4-ASK and 8-ASK modulation schemes, which are shown in Fig. 4 and 5, respectively. It is crucial to note that the selection of m_{th} is guided by ensuring the tag meets the operational requirements of the BackCom system. We observe that $P_{L,avg}^*$ increases with $\mathcal{P}^{\{1\}}$, which implies the significance of considering the transmit symbols' probability in the tag design. To understand how it improves $P_{L,avg}^*$, we study the underlying optimal reflection coefficient Γ_{ai}^* of each state. Fig. 6(a) and 6(b) illustrate Γ_{ai}^* versus $\mathcal{P}^{\{1\}}$ with different m_{th} for 4-ASK and 8-ASK, respectively. The Γ_{ai}^* corresponding to the symbol with a relatively higher occurrence probability is closer to 0, resulting in higher P_{Li} and thereby increasing $P_{L,avg}^*$.

On the other hand, the BackCom system's SER performance depends on m_{th} as given in (7). To illustrate this relationship, we plot the SER for various values of m_{th} and different transmission distances in Fig. 7, visually demonstrating the impact of m_{th} on the SER. It is evident that the SER decreases with higher m_{th} , resulting in reliable BackCom. In Fig. 4 and 5, we observed a decrease in $P_{L,avg}^*$ with an increase in m_{th} . This is because it requires a greater mismatch degree of Γ_{ai}^* to achieve the high m_{th} , thereby reducing P_{Li} in each state and drops $P_{L,avg}^*$ in the sense.

As the passive tag relies on harvesting energy from the reader's broadcasted signal, the transmission distance between the reader and the tag emerges as a crucial factor influencing the tag's harvesting power. Generally, the transmitted signal's energy experiences a significant decrease over propagation distance. In consideration of this, we set $m_{th} = 0.05$, $P_{b,min} = 5\mu\text{W}$, and $M = 8$ to plot $P_{L,avg}^*$ against d , as illustrated in Fig. 8. Additionally, we show the

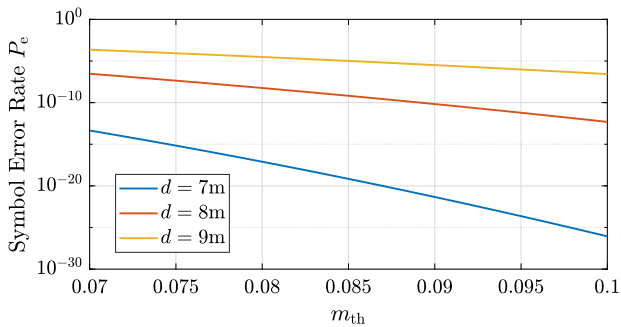


Fig. 7: Symbol error rate of BackCom system versus modulation index m_{th} for different transmission distances.

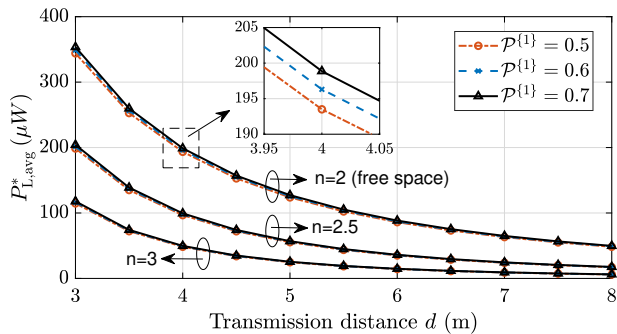


Fig. 8: $P_{L,avg}^*$ versus d at different \mathcal{P}^{1} for 8-ASK.

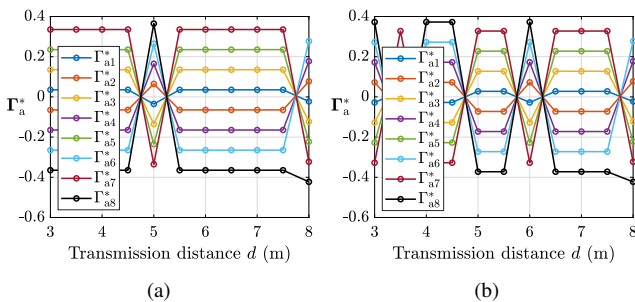


Fig. 9: Optimal Reflection coefficient for 8-ASK at (a) $\mathcal{P}^{1} = 0.6$ and (b) $\mathcal{P}^{1} = 0.7$ for $n = 3$.

impact of the path loss exponent n on $P_{L,avg}^*$ within the same plot.

Results in Fig. 8 demonstrate a substantial decrease in $P_{L,avg}^*$ as d increases, dropping to less than $6.3\mu\text{W}$ when $d = 8\text{m}$ and $n = 3$. We also observe a significant decrease in $P_{L,avg}^*$ as n increases from 2 to 2.5 and subsequently to 3. This underscores that the BackCom system environment plays a vital role in energy harvesting. The decrease in $P_{L,avg}^*$ can be attributed to the exponential attenuation of the RF carrier over the distance d and the presence of a poor propagation medium, leading to a significant reduction in P_a . Besides, the d and n exhibit a more pronounced impact on $P_{L,avg}^*$ compared to \mathcal{P}^{1} . Similarly, we plot the underlying Γ_a^* to observe how each state's reflection coefficient varies with d . Specifically, Fig. 9(a) and 9(b) depict plots for $\mathcal{P}^{1} = 0.6$ and $\mathcal{P}^{1} = 0.7$, respectively. Our observations reveal that $|\Gamma_{ai}^*|$ remains constant within a certain transmission range (up to $d = 7.5\text{m}$ in our case) and only varies beyond a specific distance ($d = 8\text{m}$ in our

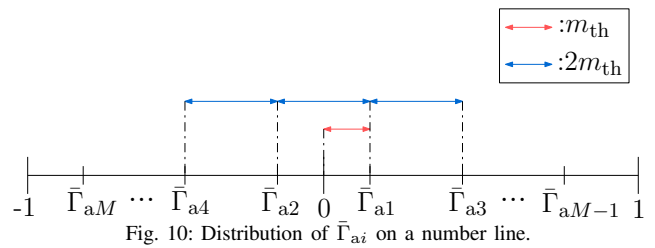


Fig. 10: Distribution of $\bar{\Gamma}_{ai}$ on a number line.

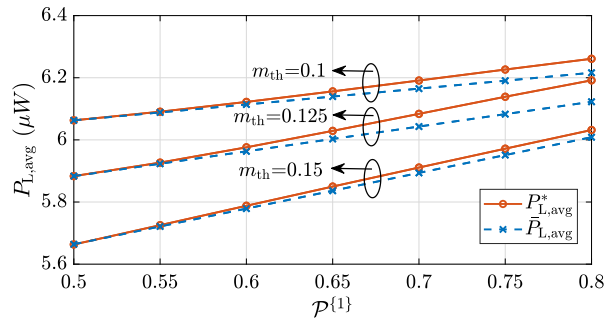


Fig. 11: $P_{L,avg}$ at different \mathcal{P}^{1} for 4-ASK.

case). This suggests that d does not influence Γ_{ai}^* within a certain range where none of the Γ_{ai}^* values are selected that just satisfy $P_{L,min}$ or $P_{b,min}$. As d increases and results in a decrease in P_a , either or both $P_{L,min}$ and $P_{b,min}$ constraints set a boundary to Γ_{ai}^* . Specifically, in Fig. 9(b), we observe that the $P_{b,min}$ constraint establishes a boundary such that $\Gamma_{ai}^* \leq 0.277$ when $d = 8\text{m}$. This underscores the significance of our optimal reflection coefficient selection algorithm in maximizing the average harvested power while ensuring the essential operational requirements for the ASK-modulated BackCom system are met.

B. Performance Comparison

1) *General Case for M-ASK*: In this study, we aim to compare our load selection method with a conventional approach, focusing on demonstrating the enhancement in $P_{L,avg}$. Recent years have seen various reflection coefficient selections for backscatter tag design, with studies such as [16]–[18] considering an equal mismatch of the reflection coefficient for the BASK modulation scheme. Adopting a similar concept, we introduce a reflection coefficient selection, denoted as $\bar{\Gamma}_{ai}$, $\forall i \in \mathbb{M}$. Specifically, $\bar{\Gamma}_{ai}$ is symmetrically placed at 0 in the descending order of p_i , with an equal separation of $2m_{th}$. Assuming $\bar{\Gamma}_{a1} > \bar{\Gamma}_{a2}$ without loss of generality, we define $\bar{\Gamma}_{ai} = m_{th} \left[1 - (-1)^i \left(i + \frac{1}{2} \left((-1)^i - 1 \right) \right) \right]$. The symmetrical distribution of $\bar{\Gamma}_{ai}$ on a number line is illustrated in Fig. 10, visualizing the mismatch degree of $\bar{\Gamma}_{ai}$ at each state. Accordingly, we define $\bar{P}_{L,avg}$ as the average harvested power determined by $\bar{\Gamma}_{ai}$ as the benchmark to highlight the merits of our optimal reflection coefficients selection.

Fig. 11 plots $P_{L,avg}^*$ and $\bar{P}_{L,avg}$ for varying \mathcal{P}^{1} and different m_{th} at $d = 8\text{m}$ and $M = 4$. The result shows that $P_{L,avg}^*$ is always greater than $\bar{P}_{L,avg}$, with the

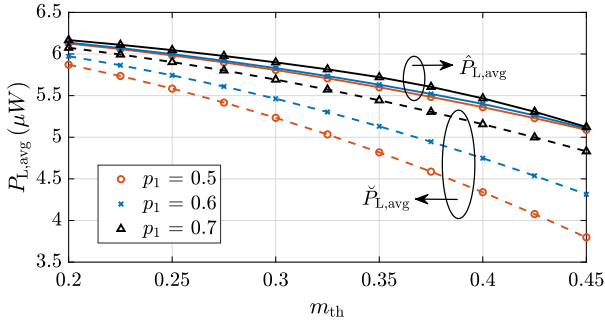


Fig. 12: $P_{L,avg}$ in BASK at different m_{th} .

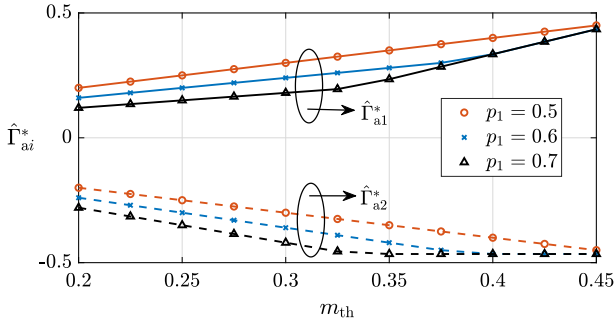


Fig. 13: $\hat{\Gamma}_{a,i}^*$ versus m_{th} .

relative improvement increasing with $\mathcal{P}^{\{1\}}$. This suggests that our optimal solution for tag design exhibits superior performance. Moreover, the symmetrical arrangement of $\hat{\Gamma}_{ai}$ imposes limitations on its application because of the asymmetrical boundary constraints of Γ_{ai} . Conversely, our algorithm offers a more adaptable and flexible reflection coefficient selection, particularly allowing a higher m_{th} .

2) *The Special Case with BASK:* As aforementioned, the BASK modulation is the most popular and widely exploited in the current backscatter tag industry, especially the RFID tag. In this context, we study the performance of our load selection with the BASK modulation scheme specified in IV-B. Additionally, we consider another prevalent load selection in BASK modulation. This involves one load in perfectly matched condition and another greatly mismatched to meet the m_{th} requirement. We denote it as $\hat{\Gamma}_{ai}$ and set $\hat{\Gamma}_{a1} > \hat{\Gamma}_{a2}$. Hence, $\hat{\Gamma}_{a1} = 0$ and $\hat{\Gamma}_{a2} = -2m_{th}$, which are used to determine the average harvested power $\check{P}_{L,avg}$.

Subsequently, we set $\check{P}_{L,avg}$ as the benchmark and graphically compare it with $\hat{P}_{L,avg}^*$, as depicted in Fig. 12. Similarly, we observed that $\hat{P}_{L,avg}^*$ decreases with m_{th} . More importantly, it is clear that $\hat{P}_{L,avg}^*$ is always greater than $\check{P}_{L,avg}$, which signifies the utility of our design. The average gain achieved by the proposed optimal reflection coefficients over the benchmark is 9.65%. Fig. 13 provides insights into the underlying $\hat{\Gamma}_{a,i}^*$, showing that $\hat{\Gamma}_{a2}^*$ reaches a constant as m_{th} increases to ensure $\hat{\Gamma}_{a2}^*$ satisfy the $P_{L,min}$ constraint.

VII. CONCLUSION

This paper provides a novel load selection for the passive backscatter tag design with the M -ASK modulation scheme that maximizes the average harvested power while meeting the tag power sensitivity, reader sensitivity, and SER

requirement. Although all the transmit symbols are generally assumed to have equal occurrence probability, we consider them unequal and are application-dependent constants in our work. We studied 2 different tag designs, where the first design is a general M -ASK modulator, and the second is a BASK modulator. Besides, we considered more comprehensive operational requirements in the former design. In contrast, the latter design neglected reader sensitivity, which is a common assumption in conventional RFID applications. We obtain global solutions in the closed-form expression with the proposed algorithms. The simulation results have shown that the symbol probability and modulation index can significantly impact the maximum average harvested power. Besides, we found that the average harvested power with the optimal load selection provided a significant average gain over the benchmark, which signifies our proposed reflection coefficients selection.

APPENDIX A PROOF OF LEMMA 2

Here, we aim to prove Lemma 2 by comparing the backscattered power at different load selections with the same harvested power. We compare the 2 considered cases, where the first case assumed the reflection coefficient $\Gamma^{(1)} = \Gamma_a^{(1)} + j\Gamma_b^{(1)}$ with $\Gamma_b^{(1)} = 0$. The second case assumed the reflection coefficient $\Gamma^{(2)} = \Gamma_a^{(2)} + j\Gamma_b^{(2)}$, with $\Gamma_a^{(2)} = 0$. Therefore, the harvested power of the first and second cases are:

$$P_L^{(1)} = \mathcal{E}_h P_a \left(1 - \left(\Gamma_a^{(1)} \right)^2 \right), \quad (\text{A.1})$$

$$P_L^{(2)} = \mathcal{E}_h P_a \left(1 - \left(\Gamma_b^{(2)} \right)^2 \right), \quad (\text{A.2})$$

and the backscattered power of these 2 cases are:

$$P_b^{(1)} = \mathcal{E}_b P_a G_r \left(1 - \Gamma_a^{(1)} \right)^2 \stackrel{(s_4)}{=} \mathcal{E}_b P_a G_r \left(2 - \frac{P_L^{(1)}}{\mathcal{E}_h P_a} + 2\sqrt{1 - \frac{P_L^{(1)}}{\mathcal{E}_h P_a}} \right), \quad (\text{A.3})$$

$$P_b^{(2)} = \mathcal{E}_b P_a G_r \left(1 + \left(\Gamma_b^{(2)} \right)^2 \right) \stackrel{(s_5)}{=} \mathcal{E}_b P_a G_r \left(2 - \frac{P_L^{(2)}}{\mathcal{E}_h P_a} \right), \quad (\text{A.4})$$

where (s_4) and (s_5) are obtained using (A.1) and (A.2), respectively. If we select the load impedance that gives $P_L^{(1)} = P_L^{(2)}$, we can clearly observe that $P_b^{(1)}$ is always greater than $P_b^{(2)}$. Hence, we proved Lemma 2.

APPENDIX B PROOF OF LEMMA 4

We determine the Hessian matrix of the objective function in problem (P4), which is given as:

$$\mathbb{H} = \begin{bmatrix} \frac{\partial^2 \hat{P}_{L,avg}}{\partial \Gamma_{a1}^2} & \frac{\partial^2 \hat{P}_{L,avg}}{\partial \Gamma_{a1} \partial \Gamma_{a2}} \\ \frac{\partial^2 \hat{P}_{L,avg}}{\partial \Gamma_{a2} \partial \Gamma_{a1}} & \frac{\partial^2 \hat{P}_{L,avg}}{\partial \Gamma_{a2}^2} \end{bmatrix} = \begin{bmatrix} -2p_1 \mathcal{E}_h P_a & 0 \\ 0 & -2(1-p_1) \mathcal{E}_h P_a \end{bmatrix}. \quad (\text{A.5})$$

Then, we find the eigenvalues of matrix \mathbb{H} , which are:

$$\lambda_{e1} = -2p_1 \mathcal{E}_h P_a, \quad (\text{A.6})$$

$$\lambda_{e2} = -2(1 - p_1) \mathcal{E}_h P_a. \quad (\text{A.7})$$

We observed that the diagonal entries of \mathbb{H} are ≤ 0 , and the determinant of \mathbb{H} being non-negative, $|\mathbb{H}| \geq 0$. Moreover, both the eigenvalues λ_{e1} and λ_{e2} are always negative. Hence, we proved that the objective function of problem (P4) is a concave function. Besides, it is noticed that constraints C2 and C10 are linear.

Next, we set $f_i = P_{L,\min} - \mathcal{E}_h P_a (1 - \Gamma_{ai}^2)$ corresponds to constraint C11. The second derivative of f_i with respect to Γ_{ai} is $\frac{\partial^2 f_i}{\partial \Gamma_{ai}^2} = 2\mathcal{E}_h P_a \geq 0$, which implies constraint C11 is convex. Since the objective function is concave, and the constraints C2, C10, and C11 are either linear or convex, we can conclude that problem (P4) is a convex optimization problem. Hence, we proved Lemma 4.

REFERENCES

- [1] A. C. Y. Goay, D. Mishra, and A. Seneviratne, "BER-aware backscattering design for energy maximization at RFID passive tag," *Infocommunications J.*, vol. 14, no. 4, pp. 49–55, 2022.
- [2] J.-P. Niu and G. Y. Li, "An overview on backscatter communications," *J. commun. inf. netw.*, vol. 4, no. 2, pp. 1–14, 2019.
- [3] H. Landaluze, L. Arjona, A. Perallos, F. Falcone, I. Angulo, and F. Muralter, "A review of IoT sensing applications and challenges using RFID and wireless sensor networks," *Sensors*, vol. 20, no. 9, 2020.
- [4] U. S. Toro, K. Wu, and V. C. M. Leung, "Backscatter wireless communications and sensing in green internet of things," *IEEE Trans. Green Commun. Netw.*, vol. 6, no. 1, pp. 37–55, 2022.
- [5] A. C. Y. Goay, D. Mishra, Y. Shi, and A. Seneviratne, "Throughput and energy aware range maximization in cooperative backscatter communication systems," in *Proc. IEEE 95th VTC2022-Spring*, 2022, pp. 1–6.
- [6] M. Kaur, M. Sandhu, N. Mohan, and P. S. Sandhu, "RFID technology principles, advantages, limitations & its applications," *Int. J. Electr. Comput. Eng.*, vol. 3, no. 1, p. 151, 2011.
- [7] R. Want, "An introduction to RFID technology," *IEEE Pervasive Comput.*, vol. 5, no. 1, pp. 25–33, 2006.
- [8] X. Lu, D. Niyato, H. Jiang, D. I. Kim, Y. Xiao, and Z. Han, "Ambient backscatter assisted wireless powered communications," *IEEE Wireless Commun.*, vol. 25, no. 2, pp. 170–177, 2018.
- [9] C. Jing, Z. Luo, Y. Chen, and X. Xiong, "Blind anti-collision methods for RFID system: a comparative analysis," *Infocommunications J.*, vol. 12, no. 3, pp. 8–16, 2020.
- [10] P. V. Nikitin and K. V. S. Rao, "Performance limitations of passive UHF RFID systems," in *Proc. IEEE APSIS*, 2006, pp. 1011–1014.
- [11] F. Muralter, H. Landaluze, R. Del-Rio-Ruiz, and A. Perallos, "Selecting impedance states in a passive computational RFID tag backscattering in PSK," *IEEE Microw. Wireless Compon. Lett.*, vol. 29, no. 10, pp. 680–682, 2019.
- [12] A. C. Y. Goay, D. Mishra, and A. Seneviratne, "ASK modulator design for passive RFID tags in backscatter communication systems," in *Proc. IEEE WAMICON*, 2022, pp. 1–4.
- [13] G. De Vita and G. Iannaccone, "Design criteria for the RF section of UHF and microwave passive RFID transponders," *IEEE Trans. Microw. Theory Tech.*, vol. 53, no. 9, pp. 2978–2990, 2005.
- [14] N. Fasarakis-Hilliard, P. N. Alevizos, and A. Bletsas, "Coherent detection and channel coding for bistatic scatter radio sensor networking," *IEEE Trans. Commun.*, vol. 63, no. 5, pp. 1798–1810, 2015.
- [15] K. V. S. Rao, P. V. Nikitin, and S. F. Lam, "Impedance matching concepts in RFID transponder design," in *Proc. IEEE Workshop on AutoID*, 2005, pp. 39–42.
- [16] A. Bletsas, A. G. Dimitriou, and J. N. Sahalos, "Improving backscatter radio tag efficiency," *IEEE Trans. Microw. Theory Tech.*, vol. 58, no. 6, pp. 1502–1509, 2010.
- [17] P. V. Nikitin, K. V. S. Rao, S. Lam, V. Pillai, R. Martinez, and H. Heinrich, "Power reflection coefficient analysis for complex impedances in RFID tag design," *IEEE Trans. Microw. Theory Tech.*, vol. 53, no. 9, pp. 2721–2725, 2005.
- [18] P. V. Nikitin, K. Rao, and R. D. Martinez, "Differential RCS of RFID tag," *Electron. Lett.*, vol. 43, no. 8, pp. 431–432, 2007.
- [19] U. Karthaus and M. Fischer, "Fully integrated passive UHF RFID transponder IC with 16.7 μ w minimum RF input power," *IEEE J. Solid-State Circuits*, vol. 38, no. 10, pp. 1602–1608, 2003.
- [20] G. Khadka, M. Nemati, X. Zhou, and J. Choi, "Index modulation in backscatter communication for IoT-sensor-based applications: A review," *IEEE Sensors J.*, vol. 22, no. 22, pp. 21 445–21 461, 2022.
- [21] J. Qian, A. N. Parks, J. R. Smith, F. Gao, and S. Jin, "IoT communications with M -PSK modulated ambient backscatter: Algorithm, analysis, and implementation," *IEEE Internet Things J.*, vol. 6, no. 1, pp. 844–855, 2019.
- [22] Q. Tao, C. Zhong, K. Huang, X. Chen, and Z. Zhang, "Ambient backscatter communication systems with MFSK modulation," *IEEE Trans. on Wireless Commun.*, vol. 18, no. 5, pp. 2553–2564, 2019.
- [23] S. Thomas and M. S. Reynolds, "QAM backscatter for passive UHF RFID tags," in *Proc. IEEE RFID*, 2010, pp. 210–214.
- [24] C. Boyer and S. Roy, "Coded QAM backscatter modulation for RFID," *IEEE Trans. Commun.*, vol. 60, no. 7, pp. 1925–1934, 2012.
- [25] Z. Niu, W. Wang, and T. Jiang, "Spatial modulation for ambient backscatter communications: Modeling and analysis," in *Proc. IEEE GLOBECOM*, 2019, pp. 1–6.
- [26] A. H. Raghavendra, A. K. Kowshik, S. Gurugopinath, S. Muhaidat, and C. Tellambura, "Generalized space shift keying for ambient backscatter communication," *IEEE Trans. Commun.*, vol. 70, no. 8, pp. 5018–5029, 2022.
- [27] J. Kimionis, A. Bletsas, and J. N. Sahalos, "Increased range bistatic scatter radio," *IEEE Trans. Commun.*, vol. 62, no. 3, pp. 1091–1104, 2014.
- [28] A. C. Y. Goay, D. Mishra, and A. Seneviratne, "Throughput maximization for multi-hop T2T backscatter communications in cooperative IoT," in *Proc. IEEE WCNC*, 2023, pp. 1–6.
- [29] J. Kimionis, A. Georgiadis, A. Collado, and M. M. Tentzeris, "Enhancement of RF tag backscatter efficiency with low-power reflection amplifiers," *IEEE Trans. Microw. Theory Tech.*, vol. 62, no. 12, pp. 3562–3571, 2014.
- [30] C. Boyer and S. Roy, "Backscatter communication and RFID: Coding, energy, and MIMO analysis," *IEEE Trans. Commun.*, vol. 62, no. 3, pp. 770–785, 2014.
- [31] D. Mishra and E. G. Larsson, "Sum throughput maximization in multi-tag backscattering to multiantenna reader," *IEEE Trans. Commun.*, vol. 67, no. 8, pp. 5689–5705, 2019.
- [32] K. Finkenzeller, *RFID handbook: fundamentals and applications in contactless smart cards, radio frequency identification and near-field communication*. John Wiley & sons, 2010.
- [33] H. Wu, Y. Zeng, J. Feng, and Y. Gu, "Binary tree slotted aloha for passive RFID tag anticollision," *IEEE Trans. Parallel Distrib. Syst.*, vol. 24, no. 1, pp. 19–31, 2013.
- [34] S. A. Tegos, P. D. Diamantoulakis, A. S. Lioumpas, P. G. Sarigiannidis, and G. K. Karagiannidis, "Slotted ALOHA with NOMA for the next generation IoT," *IEEE Trans. Commun.*, vol. 68, no. 10, pp. 6289–6301, 2020.
- [35] K. Kurokawa, "Power waves and the scattering matrix," *IEEE Trans. Microw. Theory Tech.*, vol. 13, no. 2, pp. 194–202, 1965.
- [36] P. N. Alevizos and A. Bletsas, "Sensitive and nonlinear far-field RF energy harvesting in wireless communications," *IEEE Trans. Wireless Commun.*, vol. 17, no. 6, pp. 3670–3685, 2018.
- [37] K. Haneda *et al.*, "5G 3GPP-like channel models for outdoor urban microcellular and macrocellular environments," in *Proc. IEEE VTC Spring*, 2016, pp. 1–7.
- [38] J. B. Andersen, T. S. Rappaport, and S. Yoshida, "Propagation measurements and models for wireless communications channels," *IEEE Commun. Mag.*, vol. 33, no. 1, pp. 42–49, 1995.
- [39] M. J. Feuerstein, K. L. Blackard, T. S. Rappaport, S. Y. Seidel, and H. H. Xia, "Path loss, delay spread, and outage models as functions of antenna height for microcellular system design," *IEEE Trans. Veh. Technol.*, vol. 43, no. 3, pp. 487–498, 1994.
- [40] G. R. MacCartney and T. S. Rappaport, "Rural macrocell path loss models for millimeter wave wireless communications," *IEEE J. Sel. Areas Commun.*, vol. 35, no. 7, pp. 1663–1677, Jul. 2017.
- [41] A. P. Sample, D. J. Yeager, P. S. Powledge, A. V. Mamishev, and J. R. Smith, "Design of an RFID-based battery-free programmable sensing platform," *IEEE Trans. Instrum. Meas.*, vol. 57, no. 11, pp. 2608–2615, 2008.
- [42] L. Shi, R. Q. Hu, J. Gunther, Y. Ye, and H. Zhang, "Energy efficiency for RF-powerback backscatter networks using HTT protocol," *IEEE Trans. Veh. Technol.*, vol. 69, no. 11, pp. 13 932–13 936, 2020.

- [43] X. Lu, P. Wang, D. Niyato, D. I. Kim, and Z. Han, "Wireless charging technologies: Fundamentals, standards, and network applications," *IEEE Commun. Surveys Tuts.*, vol. 18, no. 2, pp. 1413–1452, 2016.
- [44] A. C. Y. Goay, D. Mishra, R. Murch, and A. Seneviratne, "Tag antenna structure calibrated backscattering signal detection," in *Press. IEEE ICASSP*, Apr. 2024, pp. 1–5.
- [45] F. Fuschini, C. Piersanti, F. Paolazzi, and G. Falciaesecca, "Analytical approach to the backscattering from UHF RFID transponder," *IEEE Antennas Wireless Propag. Lett.*, vol. 7, pp. 33–35, 2008.
- [46] P. Nikitin and K. V. S. Rao, "Theory and measurement of backscattering from RFID tags," *IEEE Antennas Propag. Mag.*, vol. 48, no. 6, pp. 212–218, 2006.
- [47] F. Fuschini, C. Piersanti, F. Paolazzi, and G. Falciaesecca, "On the efficiency of load modulation in RFID systems operating in real environment," *IEEE Antennas Wireless Propag. Lett.*, vol. 7, pp. 243–246, 2008.
- [48] F. Yang, K. Yan, Q. Xie, and J. Song, "Non-equiprobable APSK constellation labeling design for BICM systems," *IEEE Commun. Lett.*, vol. 17, no. 6, pp. 1276–1279, 2013.
- [49] L. Wei, "Optimized M-ary orthogonal and bi-orthogonal signaling using coherent receiver with non-equal symbol probabilities," *IEEE Commun. Lett.*, vol. 16, no. 6, pp. 793–796, 2012.
- [50] S. Naderiparizi, Z. Kapetanovic, and J. R. Smith, "Wispcam: An RF-poweblack smart camera for machine vision applications," in *Proc. Int. Workshop Energy Harvesting Energy Neutral Sens. Syst.*, 2016, pp. 19–22.
- [51] *ImpinJ Speedway Reader Overview, Software Tools, Accessories, and Specifications*, IMPINJ, 2023, version 2.5. [Online]. Available: https://www.cisper.nl/datasheets/impinj/Impinj_Speedway_Reader_datasheet.pdf
- [52] J. Miranda, R. Abrishambaf, T. Gomes, P. Gonçalves, J. Cabral, A. Tavares, and J. Monteiro, "Path loss exponent analysis in wireless sensor networks: Experimental evaluation," in *Proc. IEEE INDIN*, 2013, pp. 54–58.